Master in Chemical Engineering

Development of tools to automate 3D model designs in Autodesk Inventor from Microsoft Excel spreadsheet

A Master's dissertation

by

Pedro Filipe Monteiro da Cruz

Developed within the course of dissertation

held in

Advanced Cyclone Systems



Supervisor at FEUP: **Professor Romualdo Luís Ribera Salcedo**

Supervisor at Advanced Cyclone Systems: **Doctor Júlio José da Silva Paiva**



Departamento de Engenharia Química

July of 2019

CLASSIFIED DOCUMENT. USE ONLY FOR EVALUATION PURPOSES

Acknowledgment

Ao Eng. Dr. Júlio Paiva, como orientador na Advanced Cyclone Systems, o meu agradecimento pela oportunidade dada, por toda a ajuda prestada neste processo, bem como a confiança demonstrada em mim ao longo de todo o trabalho, tendo sido dadas todas as condições para que conseguisse cumprir e ultrapassar os objetivos.

Ao Prof. Dr. Romualdo Salcedo, como orientador na Faculdade de Engenharia da Universidade do Porto, o meu obrigado pela oportunidade fornecida, confiança no meu trabalho e disponibilidade demonstrada.

À Eng. Joana Rocha e ao Carlos Reis, o meu profundo agradecimento por toda a ajuda, tempo despendido e companheirismo no tempo passado na ACS. Foram fatores fundamentais para a conclusão deste trabalho.

A todo o resto da equipa ACS, que me fizeram sempre sentir bem-vindo, que nunca perderam uma oportunidade de me ajudar, e pelos momentos (bem) passados, o meu sincero obrigado.

Um agradecimento a todo o corpo docente e não docente do MIEQ e da DTU, que me ajudaram neste percurso. Foi com eles que aprendi muito do que fazer e do que não fazer. Um obrigado especial ao Professor Fernando Martins, Professor José Miguel Loureiro, Professor John M. Woodley e ao Professor Manuel Pinelo, que me ensinaram a pensar como um engenheiro.

Um grande obrigado a todos os colegas que comigo viveram o dia a dia neste curso, em especial à Catarina, Helena, Marta e Zé. Estiveram comigo nos tempos mais difíceis, mas também nos melhores!

Agradeço também aos meus amigos fora da faculdade, em especial à Ana, que me ajudaram sempre no que foi preciso e por estarem sempre lá, mesmo quando estavam longe.

Palavras não fazem jus ao quão agradecido estou, mas um super obrigado à Rita. Sem ela, tenho a certeza que não estaria nesta posição. Manteve-me na rota, mesmo quando parecia impossível. Deu-me a força de vontade necessária para superar as dificuldades que surgiram.

Por último, o meu obrigado à minha família, com especial foco nos meus pais. Não foi fácil, não foi previsível, foi contra corrente, mas respeitaram e apoiaram as minhas decisões sempre com ações, não apenas com palavras. Todos os dias penso que o vosso apoio foi incrível, mesmo quando nada o fazia merecer. Muito obrigado.

A todos, o meu sincero obrigado!

Abstract

The following work is a master's dissertation about cyclone systems. Its focus is on parts design and parametrization using *Autodesk Inventor* linked with a *Microsoft Excel* spreadsheet, automation of assemblies of commercialized combinations and automation of pressure drop calculations, in order to choose the best solution according to a client's request.

To meet the client's requirements, it was decided (using a proprietary computer model) that 16 cyclones of MK type would be the best solution. As of now, ACS has 4 different possible combinations of 16 cyclones, therefore a comparison between the four was made. As such, all of them had to be designed, in order to obtain all of the geometric dimensions to export and use in the pressure drop calculations.

In conclusion, by pressure drop alone, the best solution presented between the four, was the 1L-8B-2MK with an average pressure drop of 2149 Pa, although two other configurations were close enough. The final choice considered other factors, such as transport logistics and parts price, in choosing the best combination for the client.

Keywords: Automation; Cyclone; Design

Declaration

I hereby declare, on my word of honor, that this work is original and that all non-original contributions were properly referenced with source identification.

Sign and date

Index

1 Introduction 1
1.1 Framework 1
1.2 Cyclones 1
1.3 Pressure drop in a system 3
1.3.1. Duct systems losses 5
1.4 Advanced Cyclone Systems 6
1.5 Contributions of the Work 7
1.6 Organization of the thesis 7
1.6.1 Introduction 7
1.6.2 Context and State of the art 7
1.6.3 Materials and Methods 7
1.6.4 Results and discussion 7
1.6.5 Conclusion 8
1.6.6 Assessment of the work done 8
2 Context and State of the art 9
3 Materials and Methods 12
3.1 1L-16B-1MK 17
3.2 1L-8B-2MK 17
3.3 1L-4B-4MK 18
3.4 2L-4B-4MK 18
4 Results and discussion 20
4.1 Design 20
4.2 Pressure Drop Calculations 22
4.2.1 Algorithm 23
4.2.2 Combination comparison 26
5 Conclusion 29
6 Assessment of the work done 30

6.1 Objectives Achieved 30
6.2 Other Work Carried Out 30
6.3 Limitations and Future Work 30
6.4 Final Assessment 30
References 31
Appendix A1

List of Figures

Figure 1 - Cyclone Geometry Parameters. Adapted from Alves, André & Paiva, Julio & Salcedo, Romualdo. (2015). Cyclone optimization including particle clustering. Powder Technology... 2

Figure 2 - Efficiency vs flow rate. Adapted from Yu, Jianfeng & Zhang, Ting & Qian, Jianming. (2011). Efficiency testing methods for centrifugal fans. Electrical Motor Products, 125-172. Woodhead Publishing. Copyright 2011 by Woodhead Publishing [7] 3

Figure 3 - Example of a combination designed at ACS.....10

Figure 4 - Cyclone's schematic in a 1L-16B-1MK layout 13

Figure 5 - Cyclone's schematic in a 1L-8B-2MK layout 13

Figure 6 - Cyclone's schematic in a 1L-4B-4MK layout 13

Figure 7 - Cyclone's schematic in a 2L-4B-4MK layout 13

Figure 8 - Parameters link between Autodesk Inventor and Microsoft Excel.....15

Figure 9 – Path 1 in 1L-4B-4MK layout.....16

Figure 10 - Path 1 in 1L-4B-4MK layout – outlet pipeline 16

Figure 11 - Overhead collector design made using Autodesk Inventor 20

Figure 12 - 1L-2B-4HR combination 22

Figure 13 - Algorithm to calculate pressure drop in a part 24

Figure A. 1 - CD3-9. Adapted from 2001 ASHRAE handbook [9] A1

Figure A. 2 - ED4-1. Adapted from 2001 ASHRAE handbook [9]..... A2

Figure A. 3 - ED4-2. Adapted from 2001 ASHRAE handbook [9]..... A2

Figure A. 4 - ED5-2. Adapted from 2001 ASHRAE handbook [9]..... A2

Figure A. 5 - ED5-3, DC > 250 mm. Adapted from 2001 ASHRAE handbook [9]..... A2

Figure A. 6 - ED5-6. Adapted from 2001 ASHRAE handbook [9]..... A3

Figure A. 7 - ED5-9. Adapted from 2001 ASHRAE handbook [9]..... A3

Figure A. 8 - SD5-2. Adapted from 2001 ASHRAE handbook [9]..... A4

Figure A. 9 – Wye (ED5-9) A11

Figure A. 10 – 30° elbow (CD3-9).....A11

Figure A. 11 - 90° elbow (CD3-9)..... A12

Figure A. 12 - Overhead collector for a battery comprised of 6 cyclones A12

Figure A. 13 - Dust collector for a battery comprised of 4 cyclones A13

Figure A. 14 - Dust collector for a battery comprised of 6 cyclones A13

Figure A. 15 - Diverging 30° Wye (SD5-2) A14

Figure A. 16 - Example of inlet pipelines A14

Figure A. 17 - Battery of 6 cyclones A15

Figure A. 18 - 2L-2B-4MK layout A16

Figure A. 20 - Heat Transfer algorithm A20

List of Tables

Table 1 - Design Datasheet information 9

Table 2 - Physical-chemical properties of the inlet gas 12

Table 3 - Overhead collector's design parameters 20

Table 4 - Geometry and flow rate ratio in part SD5-2_B of path 1 of 1L-4B-4MK combination 23

Table 5 - Results for SD5-2_B in path 1 of 1L-4B-4MK combination 26

Table 6 - Overall pressure drop for the paths taken by the gas in given layouts 26

Table 7 - Analysis on overall pressure drops in the different combinations 27

Table A. 1 - ASHRAE handbook nomenclature. Adapted from 2001 ASHRAE handbook [9] A1

Table A. 2 - Path taken by gas stream depending on cyclones in a 1L-16B-1MK arrange - cyclones 1 to 8 ..... A4

Table A. 3 - Path taken by gas stream depending on cyclones in a 1L-16B-1MK arrange - cyclones 9 to 16 ..... A6

Table A. 4 - Path taken by gas stream depending on cyclones in a 1L-8B-2MK arrange A7

Table A. 5 - Path taken by gas stream depending on cyclones in a 1L-4B-4MK arrange A9

Table A. 6 - Path taken by gas stream depending on cyclones in a 2L-4B-4MK A10

Table A. 7 - Path 1 of 2L-4B-4MK combination - parts geometry A16

Table A. 8 - Path 1 of 2L-4B-4MK layout - iteration 1 ..... A17

Table A. 9 - Path 1 of 2L-4B-4MK layout - iteration 2 ..... A18

Table A. 10 - Path 1 of 2L-4B-4MK layout - iteration 3 ..... A19

Notation

A	area	m^2
D_h	hydraulic diameter	mm
f	friction factor	
g	gravitational acceleration	m/s^2
k	local loss coefficient	
L	length	m
$\dot{m}$	mass flow rate	kg/h
M_i	molar mass	g/mol
p_i	pressure at "i" section	Pa
$p_{s,i}$	static pressure at "i" section	Pa
p_v	velocity pressure	Pa
Q	volumetric flow rate	m^3/h
R	molar gas constant	J/(mol.K)
Re	Reynolds' numer	
R_Q	flow rate ratio	
SD	standard deviation	
T	temperature	K
v_i	velocity at "i" section	m/s
v_s	streamline local velocity	m/s
x_i	gas fraction	
z	height difference	m
Δp	pressure drop	Pa
Δp_f	friction losses in total pressure	Pa
Δp_{se}	thermal gravity effect	Pa

Greek Letters

ϵ	material's absolute roughness factor	mm
μ	viscosity	Pa.s
η	efficiency	%
ρ	fluid density	kg/m^3
ρ_a	ambient air density	kg/m^3

Indexes

i	index
n	counter

List of Acronyms

3D	three dimensions
ACS	Advanced Cyclone Systems
DD	design datasheet
PACyc	Particle Agglomeration in Cyclones
PSD	particle size distribution
VBA	Visual Basic for Applications

1 Introduction

1.1 Framework

The work developed at Advanced Cyclone Systems (ACS) had as primary objective the creation of 3D models of parts and cyclones, using *Autodesk Inventor*, and link those files into a 3rd party program, as a way to automate their design according to the inputs of the project being developed at that time. As secondary objectives, in case the main objective was completed, were the development and automation of the whole system - inlet pipeline, cyclone and outlet pipeline – and upgrade the automation algorithm of pressure drop calculations along the system, for every combination commercialized by Advanced Cyclone Systems. Lastly, using the updated pressure drop calculations, it was also required to propose a solution for a new client's project, based on the pressure drop criteria.

1.2 Cyclones

Cyclones are extensively used for particles removal of gaseous currents in different processes from diverse industries, mainly due to low costs of manufacturing, operation and maintenance, as well as versatility in handling high temperatures and/or pressures, once built with the right material.

With the cyclone's use dissemination, it became paramount to find a way to transform these gas-solid separators in the most efficient way possible. These improvements focus, mainly, in the cyclone's geometrical ratios, to handle the decreasing imposed legal emission limits [1], as well as their wide range of applications, such as reactors, dryers and removing high-valued catalysts and pharmaceutical products. [2] Cyclones have, usually, high efficiency (up to 99%+) for particles with diameter larger than 5-10 μm. [3] Along with separation efficiency, pressure drop is a major consideration for choosing the adequate cyclone geometry, to reduce operating costs. [4]

Cyclones, conceptually, aren't complicated, as it is an equipment with a simple geometry and no moving parts. Referring to Figure 1, where a reverse-flow gas cyclone is shown, the gaseous flow enters the cylindrical chamber tangentially, through the inlet tube, and works its way down the cylinder in a downward outer vortex until it reaches the cone on the bottom, where the vortex reverses its direction of movement. The particles are separated from the gas due to centrifugal forces and are collected in some appropriate vessel located at the cone bottom. [5] The outer vortex flows upwards and the uncaptured particles exit through the exhaust duct (called vortex finder), located in the cylindrical part of the cyclone.

Traditionally, there are eight independent parameters that define a cyclone's geometry, as shown in Figure 1:

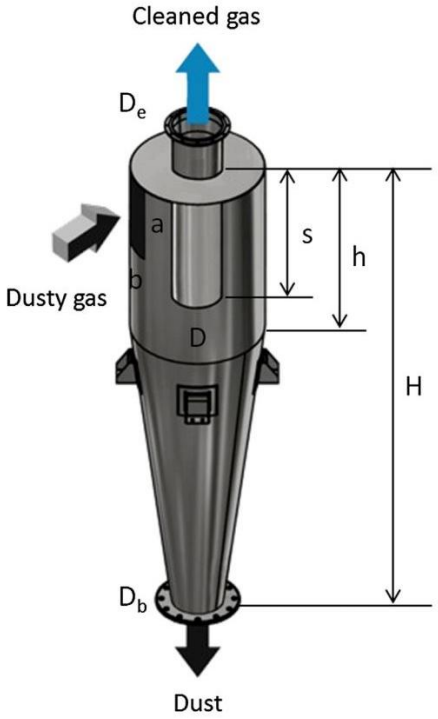


Figure 1 - Cyclone Geometry Parameters. Adapted from Alves, André & Paiva, Julio & Salcedo, Romualdo. (2015). Cyclone optimization including particle clustering. Powder Technology.

Where *a* and *b* are, respectively, height and width of the inlet tube, *D* is the cylindrical part inner diameter, *De* is the exhaust tube inner diameter, *s* is the vortex finder length, D_b is the cone's smaller diameter, *h* is the cylinder height and *H* is the cyclone's total height. Usually, all parameters are related to *D*, allowing an easier comparison between different geometrical ratios, as the cyclone geometry becomes totally defined by these 7 ratios. [6] Typically, the chosen cyclone will depend on pressure drop, particle size and desired overall efficiency of the whole process.

The calculation of pressure drop is particularly important, due to its relationship with operation costs, as shown in equation (1.1):

$$Power = \frac{\Delta p . Q}{\eta} \qquad (1.1)$$

where Δp is pressure drop (Pa), Q is volumetric flow rate (m^3/s) and η is energy efficiency of the exhaust fan/motor ensemble.

For a given cyclone diameter, a higher inlet flow rate will correspond to a higher inlet velocity, leading to an overall higher separation efficiency, but pressure drop also increases, which, in turn, increases operation costs.

In the exhaust fan/motor ensemble, there is also a flow rate value that will maximise the energetic efficiency, as shown in Figure 2.

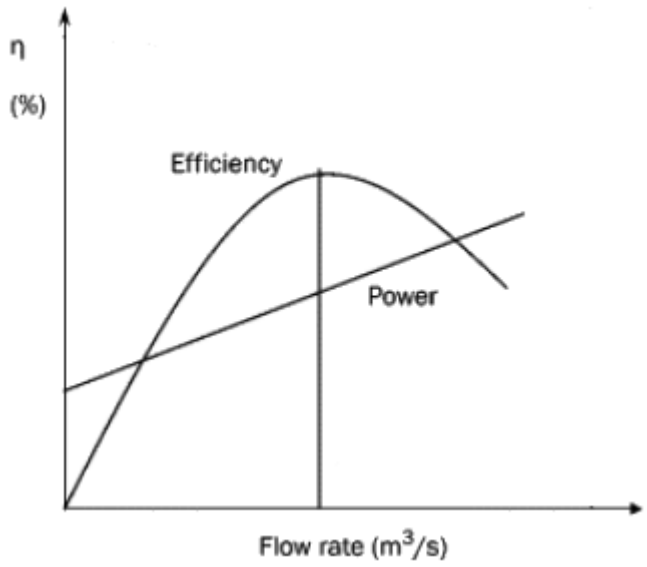


Figure 2 - Efficiency vs flow rate. Adapted from Yu, Jianfeng & Zhang, Ting & Qian, Jianming. (2011). Efficiency testing methods for centrifugal fans. Electrical Motor Products, 125-172. Woodhead Publishing. Copyright 2011 by Woodhead Publishing [7]

Therefore, a proper trade off of high separation efficiency and low pressure drop is essential to minimise the power required by the system, in order to maximise profit. [8]

1.3 Pressure drop in a system

All designs of installations regarding gas ducts must consider several factors, among others, like space availability, heat transfer and pressure drop along the system. As such, it's imperative to minimise all errors that can arise. [9]

Pressure drop is a parameter directly related with the amount of work required to operate the system at a set of conditions. As stated previously, it is important for knowing operation costs of the process, to determine economic feasibility. [8]

Considering a frictionless fluid, equating the forces of an element to the rate of change in momentum, it's possible to develop Bernoulli equation, integrate it and obtain equation (1.2) [10]

$$\frac{{v_s}^2}{2} + \int \frac{dP}{\rho} + gz = const \qquad (1.2)$$

Where v_s is streamline local velocity (m/s), P is absolute pressure (Pa), ρ is density (kg/m^3), g is gravitational acceleration (m/s^2) and z is height difference (m).

Taking fluid density as constant, equation (1.2) can be used to analyse flow in real systems. Assuming two sections (1 and 2), fluid resistance between the two can be explained by equation (1.3):

$$\frac{\rho_1 {v_1}^2}{2} + P_1 + g\rho_1 z_1 = \frac{\rho_2 {v_2}^2}{2} + P_2 + g\rho_2 z_2 + \Delta p_{t,1-2} \qquad (1.3)$$

With v_1 and v_2 being average duct velocity (m/s) (replacing streamline velocity) at section 1 and section 2, respectively, and $\Delta p_{t,1-2}$ the total pressure drop (Pa), between the 2 sections, due to friction and dynamic losses.

Given atmospheric pressure at a certain height (p_z), it is possible to add and subtract p_{z1} on the left side (regarding section 1) and p_{z2} to right side of equation (1.3) (regarding section 2), resulting in equation (1.4):

$$\frac{\rho_1 {v_1}^2}{2} + P_1 + (p_{z1} - p_{z1}) + g\rho_1 z_1 = \frac{\rho_2 {v_2}^2}{2} + P_2 + (p_{z2} - p_{z2}) + g\rho_2 z_2 + \Delta p_{t,1-2} \qquad (1.4)$$

p_z is determined using equation (1.5):

$$p_z = p_a - g\rho_a z_2 \qquad (1.5)$$

Assuming both sections have the same temperature, we can infer $\rho_1 = \rho_2$. In case there's a difference in temperature within a section, it is customary to use the average between the inlet temperature and the outlet temperature. Combining equations (1.4) and (1.5) and rearranging results in equation (1.6):

$$\Delta p_{t,1-2} = \left(p_{s,1} + \frac{\rho {v_1}^2}{2}\right) - \left(p_{s,2} + \frac{\rho {v_2}^2}{2}\right) + g(\rho_a - \rho)(z_2 - z_1) \qquad (1.6)$$

Where $p_{s,1}$ and $p_{s,2}$ are static pressure (Pa), the pressure of the ambient around the fluid, with gage at height z_1 (m) and z_2 (m), respectively; ρ_a is ambient air density (kg/m^3).

Given equations (1.7) and (1.8):

$$\Delta p = \left(p_{s,1} + \frac{\rho {v_1}^2}{2}\right) - \left(p_{s,2} + \frac{\rho {v_2}^2}{2}\right) \qquad (1.7)$$

$$\Delta p_{se} = g(\rho_a - \rho)(z_2 - z_1) \qquad (1.8)$$

with Δp being total pressure drop (Pa) and Δp_{se} being thermal gravity effect (Pa), it's possible to establish a relationship of total pressure drop, between the 2 sections, due to friction and dynamic losses, as shown in equation (1.9):

$$\Delta p_{t,1-2} - \Delta p_{se} = \Delta p \qquad (1.9)$$

Total pressure can also be calculated as shown in equation (1.10):

$$p = p_v + p_s \qquad (1.10)$$

where p_v is velocity pressure (Pa) and p_s is static pressure (Pa).

Combining equation (1.7) and equation (1.10), equation (1.11) is obtained, demonstrating how to determine p_v.

$$p_v = \frac{\rho v^2}{2} \qquad (1.11)$$

1.3.1. Duct systems losses

In every duct system, there are losses – transformation of mechanical energy into heat – and those can be either friction losses or dynamic losses.

Friction losses are a result of momentum exchanges between particles in laminar flow and particles in adjacent layers of turbulent flow, occurring along the duct, while dynamic losses result from flow instabilities caused by equipment along the system that change the airflow path's direction and/or area, thus the fluid velocity. [11]

To calculate friction losses, Darcy's equation (equation (1.12)) is used:

$$\Delta p_f = \frac{1000 f L}{D_h} \frac{\rho v^2}{2} \qquad (1.12)$$

Where Δp_f are friction losses in total pressure (Pa), f is friction factor (dimensionless), L is duct length (m), D_h is hydraulic diameter (m), v is velocity (m/s) and ρ is density (kg/m^3).

If the duct is dealing with laminar flow (Re < 2100), f is only dependant of Reynolds number. However, when dealing with fully developed turbulent flow (Re > 4000), friction factor can be calculated using Colebrook's equation [12] - equation (1.13):

$$\frac{1}{\sqrt{f}} = -2\, log\left(\frac{\varepsilon}{3.7 D_h} + \frac{2.51}{Re\sqrt{f}}\right) \qquad (1.13)$$

Where Re is Reynold's number (dimensionless) and ε is material absolute roughness factor (m).

Reynolds number can be calculated using equation (1.14):

$$Re = \frac{\rho v D_h}{\mu} \qquad (1.14)$$

with μ being dynamic viscosity (Pa.s).

Finally, for calculating dynamic losses, the value of local loss coefficient (k) is required. Using equation (1.15), k can be obtained, while equations (1.16) and (1.17) are obtained after rearranges:

$$k = \frac{\Delta p}{p_v} \qquad (1.15)$$

$$k = \frac{\Delta p}{\frac{\rho v^2}{2}} \qquad (1.16)$$

$$\Delta p = k \frac{\rho \left(\frac{Q}{A}\right)^2}{2} \qquad (1.17)$$

where Δp is total pressure drop (Pa). The value of k (dimensionless) is, usually, a given or interpolated value from literature tables, allowing total pressure drop to be calculated by multiplying velocity pressure with local loss coefficient. For linear tubes, the pressure drop is calculated per unit of length, therefore equation (1.17) must be multiplied by the length of the tube in question.

With the sum of all pressure drop values from all parts in a system, a total pressure drop is determined.

1.4 Advanced Cyclone Systems

Created in 2008, Advanced Cyclone Systems is a company specialized in developing, commercializing and installing cyclone systems custom made for the client, on a global scale, with patented technology of high efficiency cyclones. [13]

The areas of intervention range from emission control in petrochemistry and biomass industries to product recovery in pharmaceutical, chemical, food and fertilizing processes.

The proprietary technology is mainly built in three different types of cyclones – the Hurricane model, a numerical optimized cyclone; ReCyclone MH – a numerical optimized cyclone with mechanical recirculation; and ReCyclone EH – a numerical optimized cyclone with electrostatic recirculation.

1.5 Contributions of the Work

For this work, it was required to develop all parts and code to automate the design in Autodesk *Inventor*. To do such, all parameters that define a part were made to be dependent of variables existing in a *Microsoft Excel* spreadsheet so, when changing the values of these variables, the part would automatically assume the new dimensions. This spreadsheet was created and developed as part of this work, like all the code for the automations of the designs, either using *VBA* or iLogic.

In this work, the assemblies in *Autodesk Inventor* that form the combinations commercialized by ACS are also automatically generated. As such, the final cyclone layout is now possible to be tailor made for the client, using the Design spreadsheet.

For the automation of the pressure drop calculations, all of the parts parameters used are obtained from the previously mentioned spreadsheet, as well as the scripts to export into an existing pressure drop calculation spreadsheet.

1.6 Organization of the thesis

This thesis is divided into six chapters. Below is a brief description from each of them.

1.6.1 Introduction

The first chapter concerns about exposing all of objectives defined for this work. Some insight on the theoretical concepts required to understand the work developed are provided, as well as a brief presentation of the company and its areas of intervention. Is also shortly explained the contributions of the author for the developed work.

1.6.2 Context and State of the art

The second chapter explains how ACS handles a client's request, beginning with the information needed to develop a custom solution, and what kind of solutions are already in place.

1.6.3 Materials and Methods

The third chapter explains the task at hand – the client's operational requirements, the different solution options that exist, and a brief explanation of the differences between them.

1.6.4 Results and discussion

Having as input the different options presented in the previous chapter, a calculation of pressure drop algorithm is presented, along with the results for the cyclone layouts. An analysis is performed in order to help decide the best solution that fulfills the client's needs.

1.6.5 Conclusion

In this chapter, the final results and conclusions assessed from the work developed are explained.

1.6.6 Assessment of the work done

In this chapter, an evaluation of the work is done – objectives completed and final thoughts about the thesis are provided. Also presented are limitations of what has been developed as well as ongoing/future work that may be necessary.

2 Context and State of the art

The current work was developed at Advanced Cyclone Systems, S.A. (ACS), a company exclusively dedicated to the development of cyclone's technology and its commercialization. In every project, the ACS team works in close cooperation with the client, in order to understand their needs and to find the best solution. This means that every project is tailor made for the client. Of course, this also means that a lot of items will be different from project to project, making it very important to find a way to minimise the time spent in tasks, in order to meet both the product's standards, as well as the deadline set.

Presently, a client fills an inquiry, a "Design Datasheet" (DD), provided by the Commercial team, specifying the process – information about operations, purpose, type of process, etc. An example of the type of information illustrated in the DD is found in table 1:

Table 1 - Design Datasheet information

Process	Dust type	
Particles	Product Recovery/Emission Control	
	Particle Size Distribution (PSD)	
	Concentration at cyclone inlet	Maximum
		Usual
Gas and system operating conditions	Effective Gas Flow and temperature	Maximum
		Usual
		Minimum
	Atmospheric Pressure/Altitude	
	Gas Composition (% V/V)	
	Working Periods	
Target	Emissions limit/Recovery efficiency	
Layout	Space Constraints	

This information is then sent to the Technical Team. This information will serve as input in the proprietary model used by ACS - PACyc (Particle Agglomeration in Cyclones) [14]. While all the information presented in filled Design Datasheet is valuable, the main variables required to determine are the type and diameter of the cyclone, as well as total number of cyclones, together with five operational parameters: flow rate, temperature, gaseous composition at entry point, solid concentration at entry point and particle size distribution.

After the simulations are completed, with the cyclone and number of cyclones defined, the project goes through to the Engineering team. In this stage, the combination is set, according to the available area, transport logistics, operation costs and material's prices.

Additionally, a 3D design of the whole set is made, using *Autodesk Inventor*. Since there is no 3rd party link (like Microsoft Excel), this design is mostly made from the beginning, with most parts being designed as new parts every time a new project arrives, as well as having to manually input values to control the size of said parts, instead of being dependent on some variables like, e.g., flow rate.

In figure 3 is showed one of the possible combinations.

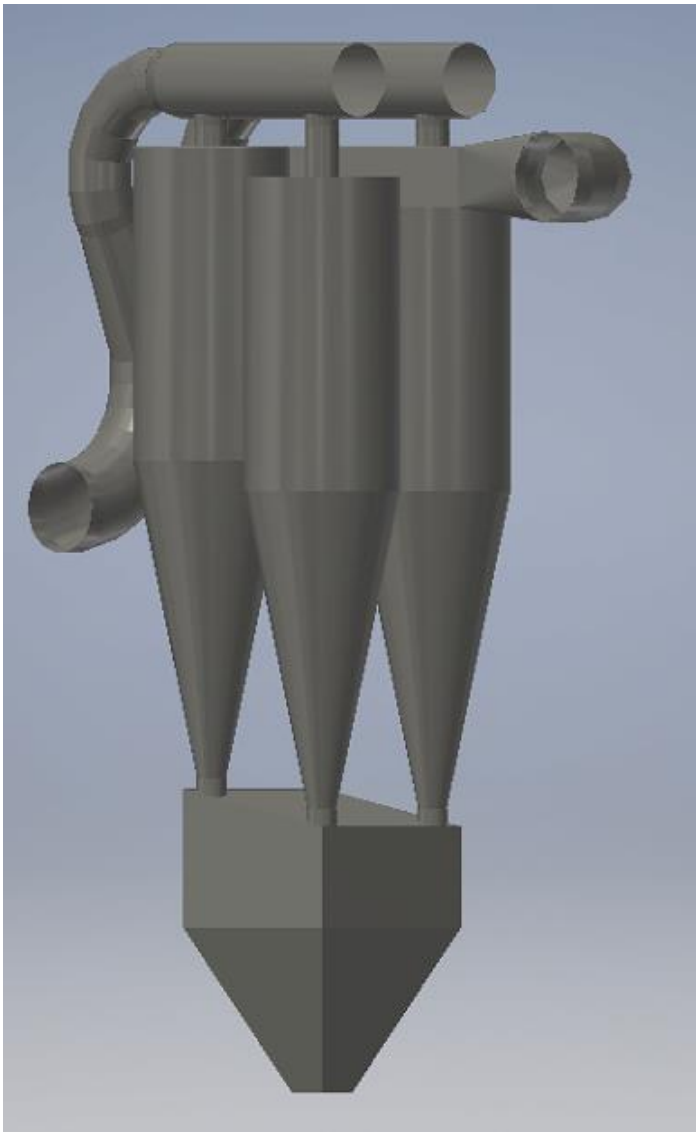


Figure 3 - Example of a combination designed at ACS

Next, with the design completed, pressure loss along the system must be calculated. Traditionally, at ACS, this is calculated using an Excel spreadsheet filled with all the parts in the system at hand (wyes, straight tubes, elbows, cyclones, along with other pieces that would be required) and geometry that characterize them – depending on the part, that could be different diameters, length and/or angles.

Due to the extensive time required to do the calculations for every cyclone in a set (specially for sets with over 16 cyclones, very commonly commercialized by ACS), pressure loss calculations for uniformity distribution estimates are usually only done in the first, middle and last cyclone in a set, since, with the experience acquired, these are, most often, the ones with the biggest difference in pressure loss. So, with the intention of balancing – put every cyclone in a set with the same pressure loss, within an acceptable margin – some changes can be made in the system, either in operational or geometrical parameters.

With this information, the 3D design is updated with the new information (in case it's needed), in order to be sent to the mechanical shop suppliers, chosen according to the clients geographical location, for the beginning of the manufacturing of the parts that will constitute the cyclone, the pipelines and structural support.

3 Materials and Methods

ACS received a client's request to handle gaseous streams from an industrial process. Using a proprietary model, with the information provided by the client in the Design Datasheet as input, it was decided that a system of 16 cyclones of MK model with 900 mm in diameter, would be the best solution for the problem presented by the client – shown in table 2.

Table 2 - Physical-chemical properties of the inlet gas

Properties	Value
Volumetric Flow Rate	25000 m^3/h
Inlet gas temperature	328 ^oC
Ambient temperature	25 ^oC
Atmospheric Pressure	101325 Pa
Inlet gas N_2 fraction	0.711
Inlet gas H_2O fraction	0.1
Inlet gas O_2 fraction	0.099
Inlet gas CO_2 fraction	0.09

As such, this work focuses in obtaining the best way to arrange the 16 cyclones, having as limitations the space available, and operations cost – directly related to pressure drop, as stated in equation [1.1].

Cyclones can be placed individually or with a set – also referred as battery. At ACS, those typical batteries are comprised of 2, 4 or 6 cyclones, and each battery in a project is similar to all the others in the layout – same cyclone type and same geometry.

Another factor to take into account when arranging the set is the number of lines – this gives information on how the cyclones/batteries are disposed, just like a line in a matrix. A single line means that every cyclones/battery are placed next to each other. Two lines means that there are cyclones/batteries that are behind another one (taking the inlet pipeline as front perspective) and share a diversion of the main pipeline.

As of now, there are five ways to arrange 16 cyclones – 16 cyclones in a line (1L-16B-1MK), each with individual entrance; 8 batteries of 2 cyclones side by side in a battery (1L-8B-2MK); 4 batteries of 4 cyclones in a single line (1L-4B-4MK); 8 batteries of 2 cyclones in two lines, one behind the other (2L-8B-2MK); and 4 batteries of 4 cyclones in two lines (2L-4B-4MK), forming a squared shape. In figures 4, 5, 6 and 7 are illustrated the layouts schematics.

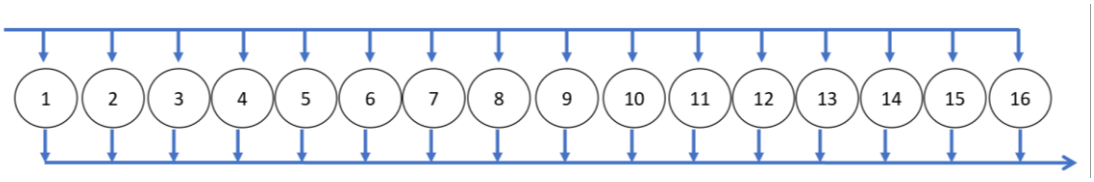


Figure 4 - Cyclone's schematic in a 1L-16B-1MK layout

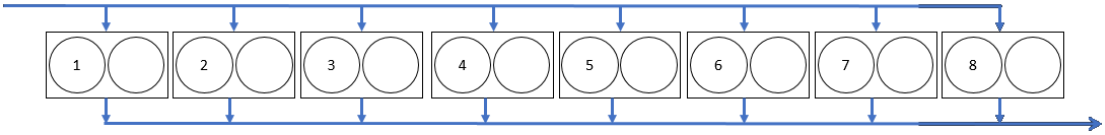


Figure 5 - Cyclone's schematic in a 1L-8B-2MK layout

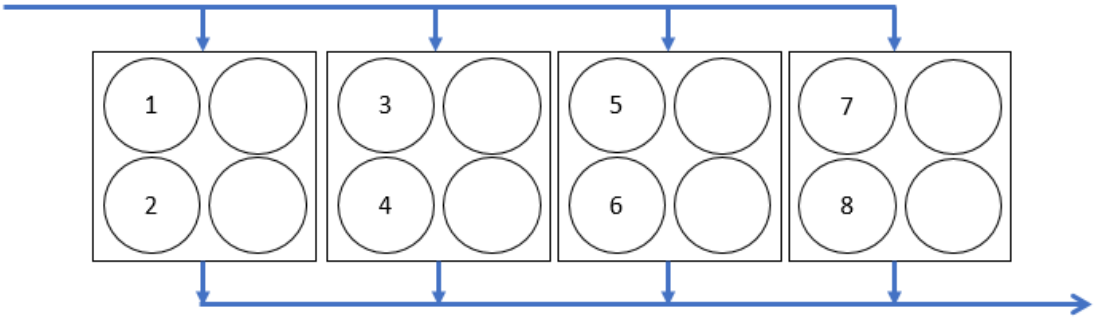


Figure 6 - Cyclone's schematic in a 1L-4B-4MK layout

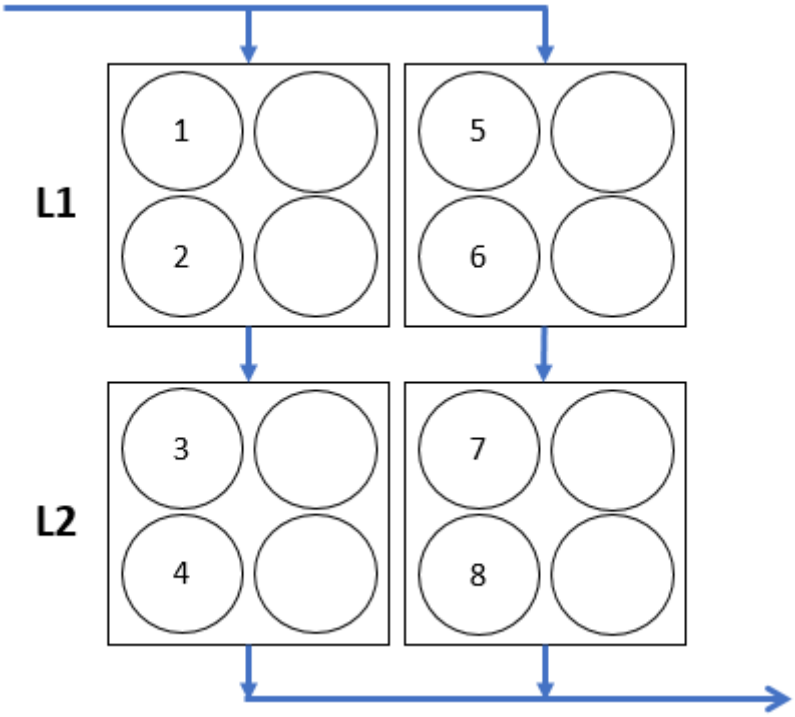


Figure 7 - Cyclone's schematic in a 2L-4B-4MK layout

Since the cyclone's type and geometry is the same in all combinations, one can assume cyclone's loss coefficient approximately the same, with the change in overall pressure drop resulting from differences in fluid density at flow rate through the path that comprises each cyclone, since the inlet duct to the outlet duct and each path is originated from the disposition and parts required in each combination. The calculation of the local loss coefficient in the cyclone is proprietary information of ACS, therefore the method will not be disclosed. However, a nominal local loss coefficient value will be provided for calculations.

The geometrical values of all parts in the system (diameters, length and radius) were all calculated having just volumetric flow rate and desired velocities at different knots along the system, assuming a constant temperature along the system, thus with volumetric flowrate constant. To calculate these values automatically, according to the combination in use and inputs required by the client, a macro (*Visual Basic for Applications* code) was developed, as well as iLogic rules to guarantee the automation of the design in *Autodesk Inventor* according to the Excel spreadsheet linked, and to export part properties from *Autodesk Inventor* to the Excel spreadsheet.

As such, template spreadsheets were created to automate all the process. The first goal was to automate the 3D models, having as little inputs as possible. To get started, all the parts that could be in a system as used in ACS were designed in *Autodesk Inventor*, with the dimensions in function of parameters in the spreadsheet. With the information on flow rate, cyclone's model and velocities in different places along the system, a spreadsheet is generated with the code to create a project folder and subfolders, copy all the parts used in a template the amount of necessary times according to the layout input, and to create parameters required to define a part (length, angle, diameters, among others) for all parts in a combination. In figure 8 illustrates the way to link *Microsoft Excel* "Design Spreadsheet" with *Autodesk Inventor*.

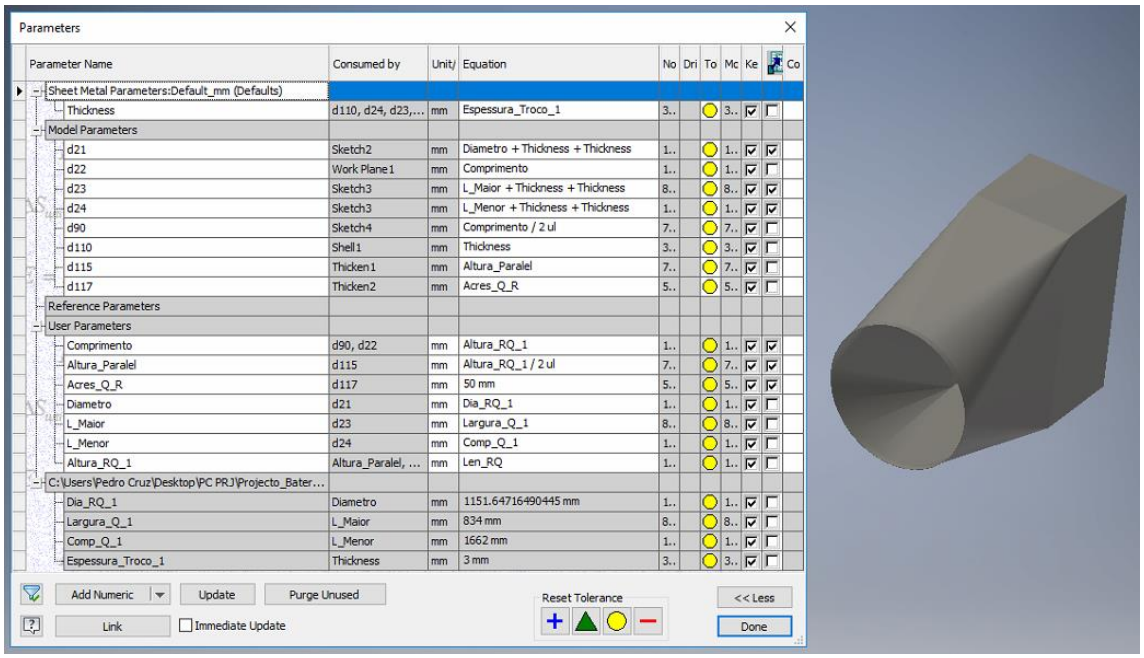


Figure 8 - Parameters link between Autodesk Inventor and Microsoft Excel

Afterwards, a different spreadsheet was created, with macros to obtain parts' parameters created in the Design Spreadsheet. In this new file, several macros were developed; and transfer the parts parameters from the Design file, with interpolation of several variables

As stated previously, automating the calculations not only expedites the process considerably, but also allows to know pressure drop in every knot along the system. Knowing the pressure loss in every part, also allows to get a real value of fluid density in every part, leading to a more accurate value of overall pressure drop, as seen in equation (3.1).

$$\rho = \frac{MP}{RT} \qquad (3.1)$$

With ρ being fluid density (kg/m^3), M is molar mass (kg/kmol), P is absolute pressure (Pa), R is molar gas constant (8314 J/(kmol.K)) and T is temperature (K).

With the aim of properly calculate and compare overall pressure drop along the system in all cyclone layouts, their differences need to be understood.

One of the main differences between the layouts is the number of parts required. In order to calculate pressure drop in every single part in the gas stream, according to the cyclone it passes through, it's imperative to define said path. With a high number of parts, a higher overall pressure drop is to be expected. In this work, the path is defined as the first knot in the inlet pipeline and the last knot at the outlet pipeline.

Taking as example the path 1 in a 1L-4B-4MK, the parts required are marked with numbers in figure 9.

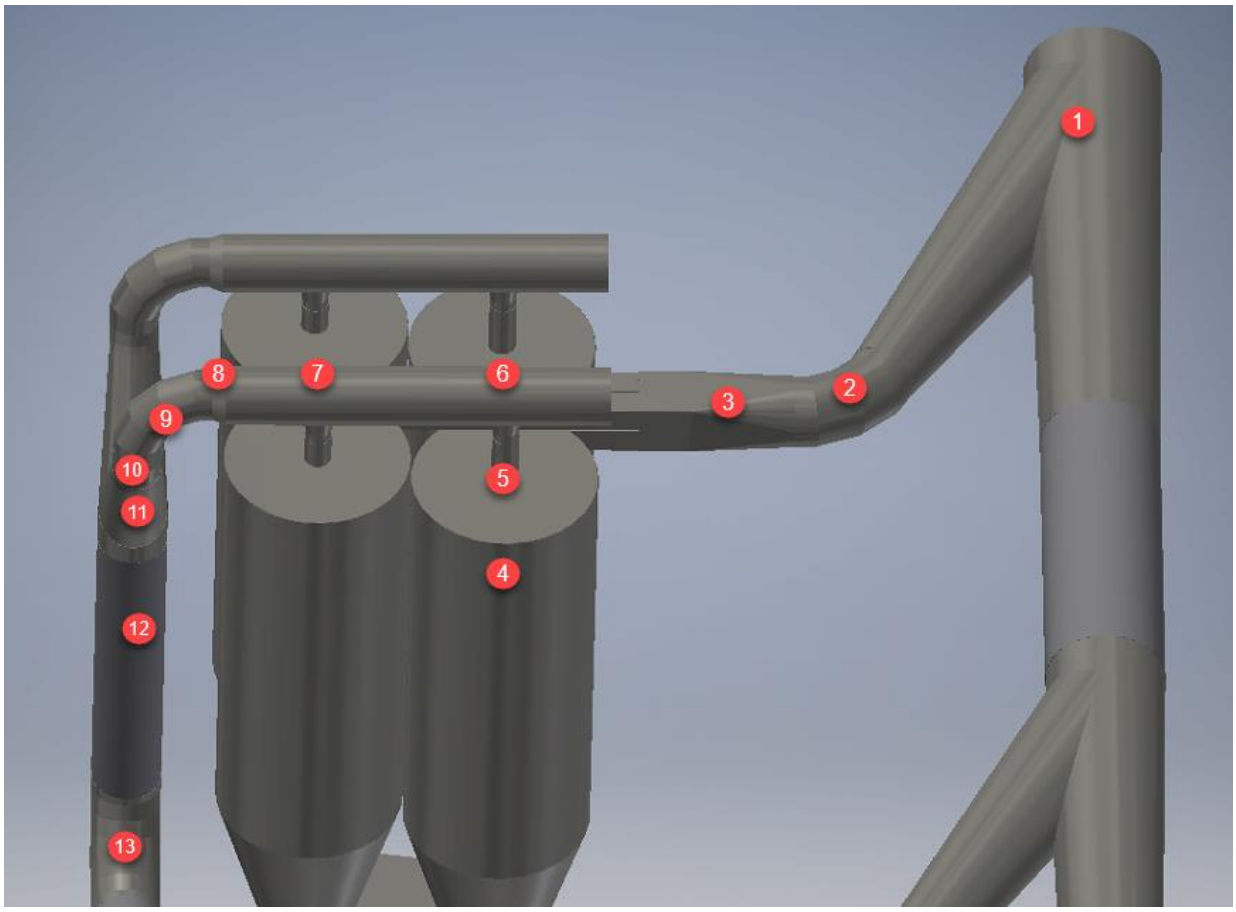


Figure 9 - Path 1 in 1L-4B-4MK layout

Where 1 is a diverging 30° wye – in path 1, the gas takes the branch part; 2 is a 60° elbow, 3 is a round to rectangular transformation, 4 is the cyclone, 5 is the cyclone's exhaust tube, 6 is a capped 90° wye, 7 is Converging 90° wye, 8 is a cone, 9 is a 90° elbow, 10 is 30° elbow, 11 is the symmetrical 60° wye, 12 is a straight tube and 13 is 90° elbow. From here, it goes through the outlet pipeline as shown in figure 10.

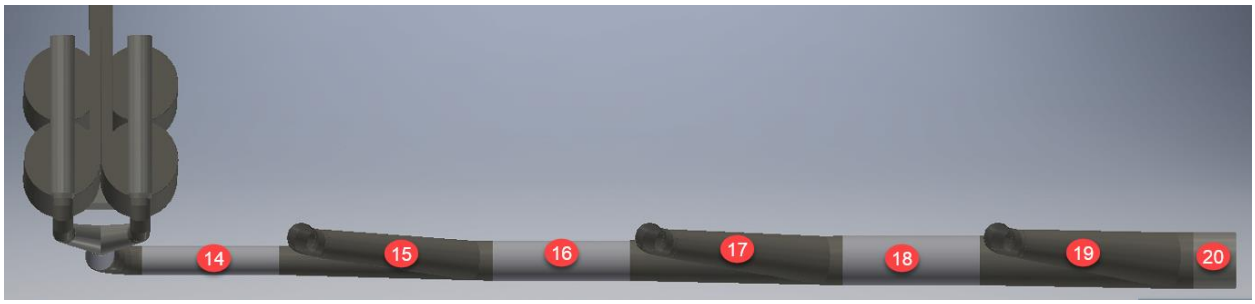


Figure 10 - Path 1 in 1L-4B-4MK layout - outlet pipeline

Where parts 14, 16, 18 and 20 are straight tubes and parts 15, 17 and 19 are converging 30° wyes.

3.1 1L-16B-1MK

In figure 4 was shown a schematic diagram of this layout, with the proper numbering. As observed, the numbering is done from left to right, with the first cyclone being the first cyclone to receive the gaseous stream.

This combination is in fact, not used, because of the area occupied and high overall pressure drop due to its immense number of required parts, increasing the number of accidents, leading (even empirically) to very unbalanced systems.

Overall, the entry pipeline and exit pipelines are comprised of 77 parts, each. Both are constituted by 30 straight circular tubes, 15 converging 30º Wyes, 15 60º elbows, 1 90º elbow. However, the entrance has 16 round to rectangular transformations and the exit pipeline has 16 cones connected to the vortex finders of the cyclones.

In tables A.2 and A.3, in appendix, all the parts according to the different paths that can be taken by the gas are shown.

All paths have a 41 part system, except for 1 and 16 (39 parts). As previously mentioned, due to its immense number of parts required, this system is expected to have the highest overall pressure drop between all the combinations being compared, most probably making it unfeasible.

3.2 1L-8B-2MK

In figure 5 was shown the enumeration in a 1L-8B-2MK layout. As observed, the numbering is from left to right. In this layout, the path in each cyclone inside a battery can be considered symmetrical, therefore the overall pressure drop is considered to be the same for left or right cyclones. Therefore, as a simplification, cyclone 1 is referring to both in the first battery, cyclone 2 is referring to both in the second battery, and so on.

The entry pipeline is comprised of 37 parts – 14 straight circular tubes, 7 converging 30º Wyes, 7 60º elbows, 1 90º elbow and 8 round to rectangular transformations.

After exiting through the exhaust tube, the gas passes through a cone, entering a 90º elbow, passing through a 30º elbow before entering the symmetric wye. In this, it converges with the gas coming from the other cyclone in the battery. Afterwards, the gas flows into the exit pipeline.

The exit pipeline has 78 parts: 15 straight circular tubes, 7 converging 30º Wyes, 7 60º elbows, 17 90º elbows, 16 30º elbows, 8 Symmetrical Converging 60º Wye and 8 round to rectangular transformations.

In table A.4 is shown the sequence of parts travelled by the gas according to the cyclone. Using this combination will require fewer parts in both cyclones in the first and last battery, compared to the rest. Overall, the gas passing through cyclones 1 and 8 will have travelled in 27 parts, while the gas passing through all the other batteries will pass through 29 parts. Therefore, a lower overall pressure drop is expected in the first and last batteries.

3.3 1L-4B-4MK

The enumeration of cyclones in a layout is done in from left to right in the line and from up to down in a column, as shown in figure 6.

As a simplification, it was decided that every pair of cyclones side by side, inside a battery, are symmetrical, therefore have a similar pressure drop.

In this combination, the entry pipeline is comprised by 17 parts in total – three diverging Wyes with 30° angle, three 60° elbows, six straight pipes, one 90° elbow and four rectangular to circular transformations.

Worth noting that cyclones located at the back of the battery have a rectangular tube as an extension. In the cyclone, the gas exits through the exhaust tube, enters the collector above and goes through until it reaches the convergent at the end, in order to increase velocity. Afterwards, it flows through a 90° and a subsequent 30° elbow, reaching a converging 60° symmetric wye. From here, the gas flows to the exit pipeline.

The exit pipeline is symmetrical to the entry pipeline, with 13 parts – three converging Wyes with 30° angle, three 60° elbows, one 90° elbow and six straight pipes. However, in the exit pipeline is also considered a straight circular tube.

In table A.5 is shown the path taken by the gas, part by part, for every cyclone in this combination.

From a preliminary analysis, a higher pressure drop is to be expected from the flow rate passing through in cyclones 3, 4, 5 and 6, since the gas flows through more parts, compared to the other cyclones in this combination.

3.4 2L-4B-4MK

In figure 7 was shown the numbering of cyclones in a 2L-4B-4MK layout.

The numbering is done from up to down, left to right. As in previous arranges presented (1L-4B-4MK), cyclones side by side are considered symmetrical.

The entry pipeline is comprised by 7 parts in total – one diverging Wye with 30° angle, one 60° elbows, two straight pipes, one 90° elbow and two rectangular to circular transformations.

The principle of operation is the same as previously explained the "1L-4B-4MK" combination. The main difference is in the size of the collector above the cyclones. In this arrange, the collector gathers the gas product of the 4 cyclones in its column. Afterwards, the current exits the collector through the transformation, passes through a 90° and a 30° elbow and reaches a converging 60° symmetric wye, where it meets the exit pipeline.

The exit pipeline is comprised of 2 converging symmetric Wye with 60° angle, 4 30° elbow, 5 90° elbows, 1 60° elbow, 1 converging Wye with 30° angle and two straight pipes – 15 parts in total.

In table A.6 is shown the path taken by the gas for every cyclone, in a 2L-4B-4MK combination.

Out of all layouts presented, this appears to be have the lowest pressure drop, as well as being the most balanced – small variance in overall pressure drop in all pathways, and just 18 to 19 parts per path.

Using equation (1.17) for every part, a value for overall pressure drop in a path can be reached. Afterwards, a comparison of the average of overall pressure drop in all layouts will allow to choose the best layout to solve the client's problem, as previously stated. These results are presented in page 27.

4 Results and discussion

4.1 Design

In order to properly design parts, it is needed to know the relationship between every single one in a given system. Therefore, in order to build a system, it is required to define the inlet flow rate and velocity in several places along the system. Most often, these places include the admission pipeline, cyclone's inlet tube, cyclone's exhaust tube, the overhead collector, and the exit pipeline.

In figure 11 is provided an example of a design made for this thesis. In this case, it is illustrated a design of the overhead collector in a battery of 4 cyclones.

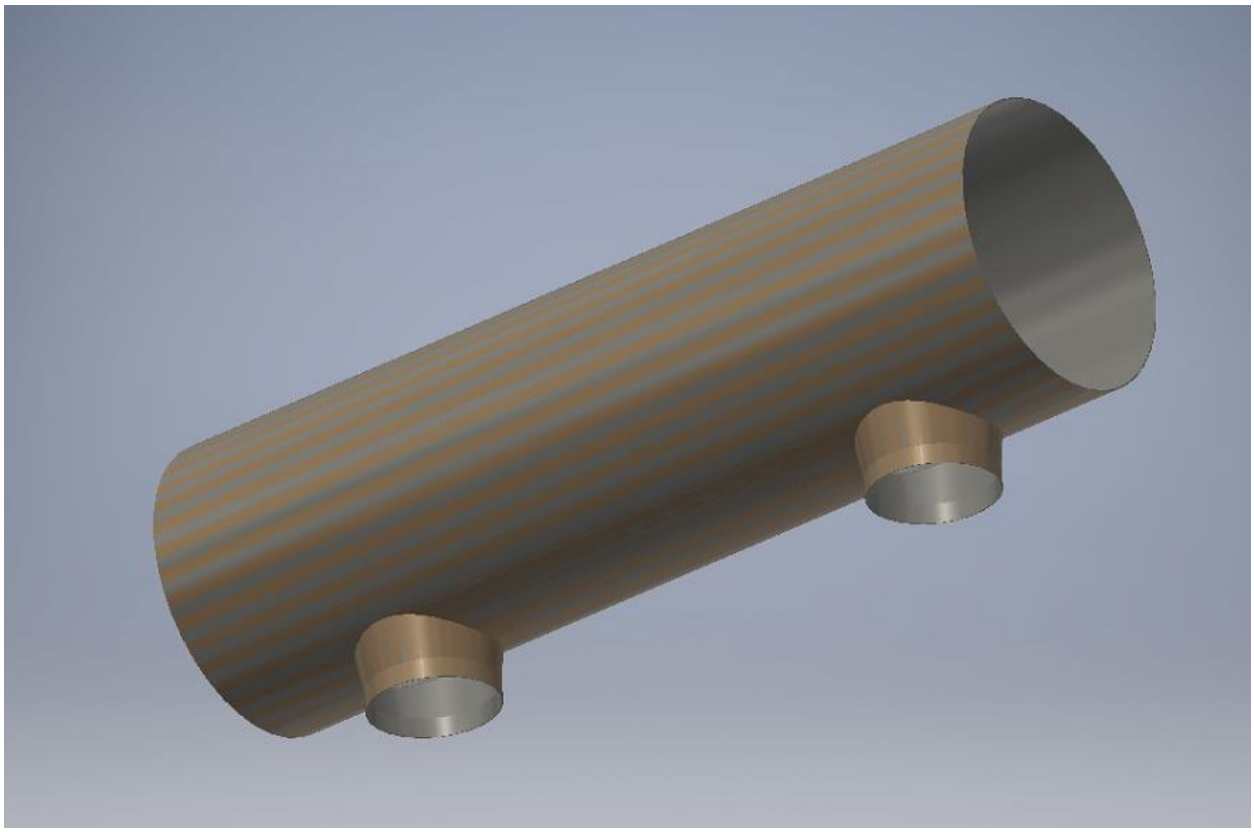


Figure 11 - Overhead collector design made using Autodesk Inventor

The overhead collector design is automated using the parameters show in table 3:

Table 3 - Overhead collector's design parameters

Parameters	Explanation
Thickness	Thickness of the sheet metal used to build the collector
Velocity	Fluid velocity at the part's exit

Number of cyclones	Number of cyclones that the collector will pass through, indicating how many inlet cones will there be in the design. In the case presented, it will pass through two cyclones
Diameter	Overhead collector diameter, calculated with the flow rate at exit and velocity desired
Cone height	Determines the height of the cone; this cone is the link between the cyclone's exhaust tube and the collector's main body and is used to slow down the fluid to lower velocities.
Cone's small diameter	This diameter is equal to the diameter of the cyclone's exhaust tube
Cone's angle	Determines the inclination of the cone
Tube height	Nominal value for the height of the neck before the cone
Distance between cyclones	Parameter to determine the separation between both holes in the collector's main body.
Cyclone's diameter	Parameter to determine the length of the ends of the collector.
Security Factor	Adds a value to both ends of the main tube, so that the length of the ends does not conflict with other parts
Distance between batteries	Parameter that will determine the length between the holes, in case there is back to back batteries in a combination, e.g. 2L-4B-4MK. In the presented figure above, that value is null

As such, after these parameters are automated and calculated in the Design Spreadsheet, the link between the *Excel* and *Inventor* is created. That way, the part is now ready to be put together with other parts and form an assembly of the combinations, as show in figure 12.

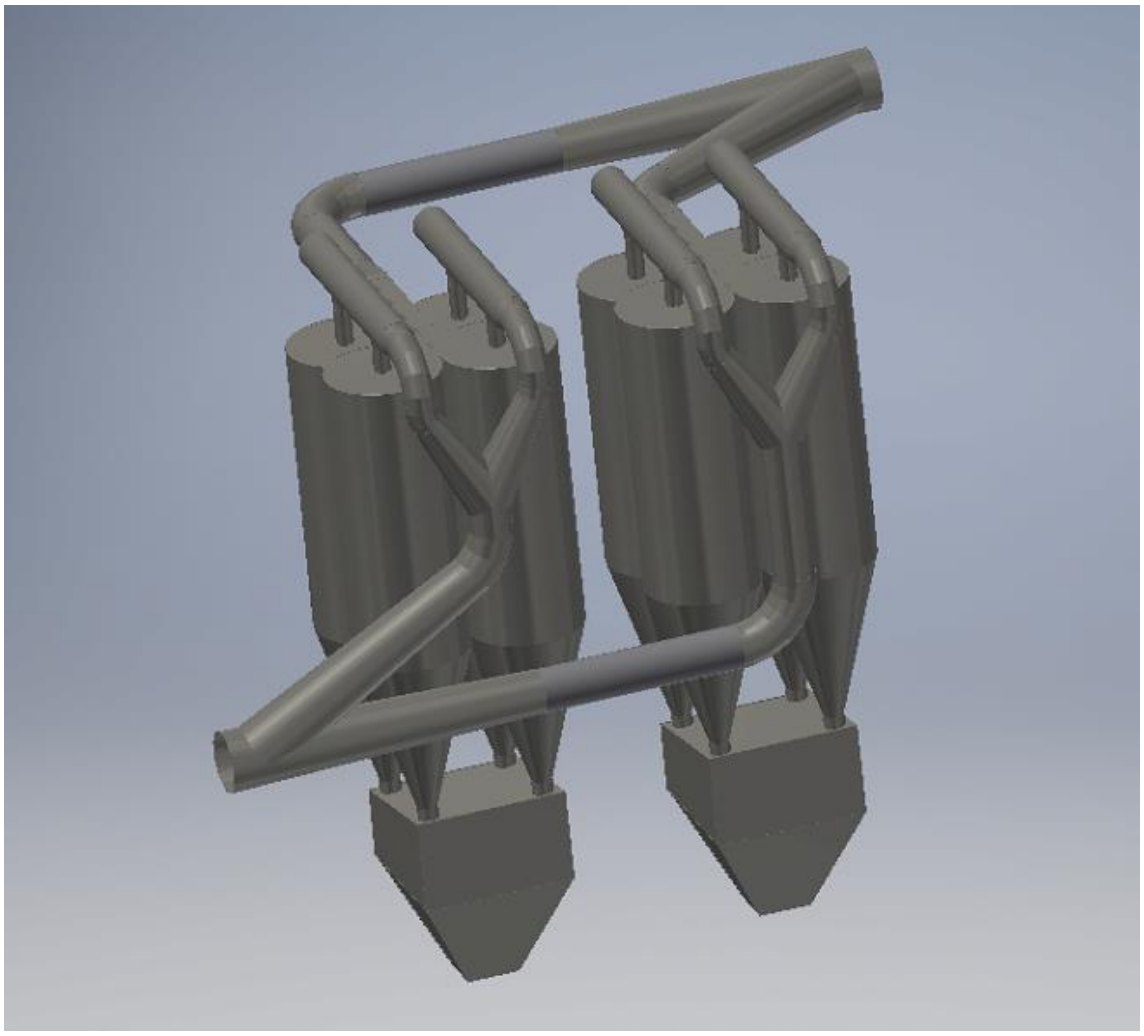


Figure 12 - 1L-2B-4HR combination

In appendix are shown a few more examples of parts and combinations designed and automated in the context of this work.

4.2 Pressure Drop Calculations

With the designs completed, it is possible to automate pressure drop calculations. All the dimensions are known and could be exported to another spreadsheet. In order to obtain an accurate value of overall pressure drop, an iterative algorithm was formulated. As such, all the calculations required will be presented, taking as an example the first part of the path 1 of the 1L-4B-4MK combination - SD5-2_B.

However, the gas molar mass must be calculated first, using equation (4.1).

$$M_T = \sum M_i \, x_i \qquad (4.1)$$

Where M_T is the gas molar mass (kg/kmol), M_i is the gas component molar mass (kg/kmol) and $\underline{x_i}$ is the gas component volume fraction (%). Having as inputs the values shown in table 2, a value of 29.39 g/mol is reached.

Fluid density is calculated using equation (3.1), with R = 8314 J/(kmol.K). Therefore, fluid density is 0.596 kg/m^3. Due to the change in fluid density along the system, volumetric flow rate will suffer changes. Consequently, it is necessary to know mass flow rate, that can be calculated using equation (4.2).

$$\dot{m} = \rho Q \qquad (4.2)$$

where $\dot{m}$ is mass flow rate (kg/h), Q is flow rate (m^3/h) and ρ is fluid density (kg/m^3).

As such, with Q = 25000 m^3/h and ρ = 0.596 kg/m^3, so $\dot{m} = 14889$ kg/h.

4.2.1 Algorithm

As previously stated, an example of calculations for the SD5-2_B in path 1 of 1L-4B-4MK combination. This part is defined as shown in table 4:

Table 4 - Geometry and flow rate ratio in part SD5-2_B of path 1 of 1L-4B-4MK combination

Variable	Value
R_Q (Flow Rate ratio entering the part)	1
R_{Qb} (Flow Rate ratio at the branch)	R_Q/(number of batteries) = 1/4
Dc (Diameter at point of entry)	664.90 mm
Db (Diameter of the branch)	332.45 mm
Ds (Diameter of the supply)	575.82 mm
Qc (Flow rate at point of entry)	25000 m^3/h
Qb (flow rate of the branch)	6250 m^3/h
Qs (flow rate of the supply)	18750 m^3/h

The SD5-2 (diverging 30° Wye) has three different diameters: Dc, inlet diameter for the fluid; Ds, located in the main tube; and Db, branch diameter, located in the diverging tube with a 30° inclination. In the following example, the focus will be on the branch tube.

In figure 13 it is pictured the algorithm to calculate pressure drop in a part.

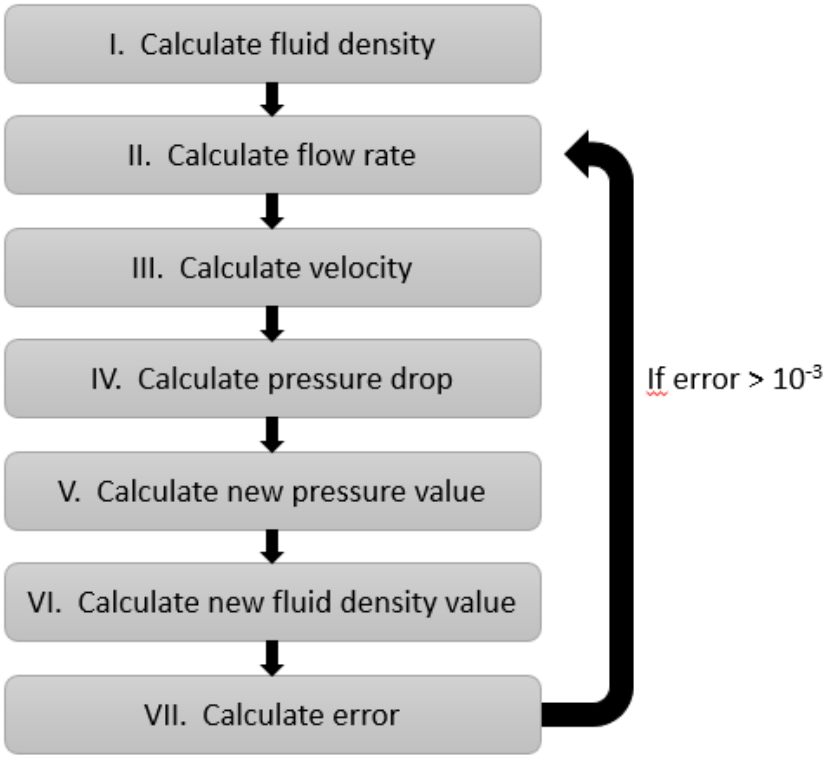


Figure 13 - Algorithm to calculate pressure drop in a part

In order to minimise errors, every part pressure drop calculation goes through, at least, 3 iterations, even if the absolute error in fluid density is smaller than 10^{-3} kg/m^3.

I. Calculate fluid density

Fluid density is calculated using equation (3.1), with R = 8314 J/(kmol.K). Therefore, ρ_1 (fluid density at first iteration) is equal to 0.596 kg/m^3.

II. Calculate flow rate

Flow rate is calculated using equation (4.3), by rearranging equation (4.2).

$$Q = \frac{\dot{m}}{\rho R_Q} \qquad (4.3)$$

Where Q is part's inlet flow rate (m^3/h), $\dot{m}$ is mass flow rate (kg/h), R_Q is Flow Rate ratio entering the part (dimensionless) and ρ is fluid density (kg/m^3).

Since the example at hand is about the first part in the system, the fluid has not been divided yet, R_Q is 1. As such, for the first iteration, flow rate at admission (Qc) is the same as the inlet flow rate of the system - 25000 m^3/h.

III. Calculate velocity

Next step is to calculate the velocity in the part. As such, equation (4.4) is used:

$$v = \frac{Q}{A} \qquad (4.4)$$

where v is velocity (m/s) and A is sectional area (m^2).

For the first iteration, with Q = 25000 m^3/h and A = 0.347 m^2, v = 20 m/s.

IV. Calculate pressure drop

Using equation (4.5), pressure drop is calculated:

$$\Delta p = k\frac{\rho v^2}{2} \qquad (4.5)$$

where Δp is total pressure drop (Pa) and k is value of local loss coefficient (dimensionless).

For the first iteration, k = 6.8625 (interpolated value), v = 20 m/s and ρ = 0.596 kg/m^3 (as previously calculated), so Δp = 817.41 Pa.

V. Calculate new pressure value

With pressure drop known, it's possible to determine a new pressure vale, by subtracting pressure drop to the original pressure value, as shown in equation (4.6):

$$p_i = p_{i-1} - \Delta p_{i-1} \qquad (4.6)$$

With the subscript i indicating the number of current iteration.

Having p_1 = 101325 Pa and Δp_1 = 817.41 Pa, the new pressure value (p_2) obtained is 100507.59 Pa.

VI. Calculate new fluid density value

As previously stated, fluid density is calculated using equation (3.1), with R = 8314 J/(kmol.K). However, for the new iteration, the value of pressure used will be pi as demonstrated in equation (4.6). For the second iteration p2 = 100507.59 Pa. Therefore, the new value of fluid density (ρ_2) is 0.591 kg/m^3.

VII. Calculate error

After obtaining the new value for fluid density, the error is calculated using equation (4.7).

$$error = \sqrt{(\rho_i - \rho_{i-1})^2} \qquad (4.7)$$

With ρ_2 = 0.5964 kg/m^3 and ρ_1 = 0.5966 kg/m^3, then error = 2x10^{-4} kg/m^3.

As previously stated, every part goes through at least three iterations so, even though the error obtained was smaller than 10^{-3}, another iteration will be calculated.

In table 5 are illustrated the values for all the variables according to the number of iterations.

Table 5 - Results for SD5-2_B in path 1 of 1L-4B-4MK combination

Iteration	p (Pa)	ρ (kg/m^3)	Q (m^3/h)	v (m/s)	Δp (Pa)	Error
1	101325.0	0.5956	25000	20.00	32.4580	
2	101292.5	0.5954	25008	20.01	32.4684	2 x 10-4
3	101292.5	0.5954	25008	20.01	32.4684	0

As can be seen, the first value of fluid density was a good approximation, and pressure drop in SD5-2_B in path 1 of 1L-4B-4MK combination is 32.4684 Pa.

4.2.2 Combination comparison

Using this algorithm for every part in all paths in all layouts, it is possible to compare all of them, and thus choose the best option for the client's process.

In table 6 is illustrated the overall pressure drop along all the paths possible in the four layouts mentioned. Due to the extensive calculations performed, for every part of every path in all combinations, only the value of the final iteration of overall pressure drop in every path in all layouts is presented. However, an example of the results obtained can be seen in the appendix section.

Table 6 - Overall pressure drop for the paths taken by the gas in given layouts

1L-16B-1MK		1L-8B-2MK		1L-4B-4MK		2L-4B-4MK	
Path	**Δp (Pa)**	**Path**	**Δp (Pa)**	**Path**	**Δp (Pa)**	**Path**	**Δp (Pa)**
1	4350.6	**1**	2079.5	**1**	2173.4	**1**	2195.8
2	4325.9	**2**	2181.1	**2**	2160.2	**2**	2193.9
3	4067.5	**3**	2112.3	**3**	2257.3	**3**	2170.9
4	3792.8	**4**	2091.2	**4**	2244.1	**4**	2146.7
5	3403.5	**5**	2171.3	**5**	2187.4	**5**	2275.0

6	2699.5	**6**	2140.1	**6**	2174.2	**6**	2273.0
7	1733.9	**7**	2179.3	**7**	2198.2	**7**	2250.0
8	1818.9	**8**	2234.6	**8**	2185.0	**8**	2225.9
9	1907.6						
10	1988.9						
11	816.8						
12	72.5						
13	-322.8						
14	-552.9						
15	-653.6						
16	-675.7						

Observing the values obtained for overall pressure drop for the 1L-16B-1MK, it can be concluded that this combination is the worst for the problem presented by the client. While, in reality, pressure drop in this combination is not negative, it provides a mathematical basis to discard this combination. A possible reason for this negative value is related to the loss coefficient in the branch part of the wye. While loss coefficient may be negative due to viscous stresses transferring energy between the two branches of a junction. [15], in this situation, it is probably related with the interpolations made to obtain the loss coefficient of the part.

Given the table above, an analysis of pressure drop values obtained is executed, to help decide which combination is best for the problem as defined previously. That analysis is shown in table 7.

Table 7 - Analysis on overall pressure drops in the different combinations

	1L-16B-1MK	1L-8B-2MK	1L-4B-4MK	2L-4B-4MK
Average (Pa)	1798.3	2148.7	2197.5	2216.4
Maximum (Pa)	4350.6	2234.6	2257.3	2275.0
Minimum (Pa)	-675.7	2079.5	2160.2	2146.7
SD (Pa)	1795.36	49.22	32.64	44.32

Where average is the sum of all pressure drop values in every path divided by the number of paths, maximum is the highest pressure drop obtained for that layout, while minimum is the lowest pressure drop in the same layout. Standard deviation (SD) is calculated using equation (4.8).

$$SD = \sqrt{\frac{\sum|x - \bar{x}|^2}{n - 1}} \qquad (4.8)$$

where *x* is the value of pressure drop in a path in a given layout, $\bar{x}$ is the average pressure drop in a layout, and *n* is the number of paths in the layout.

Therefore, taking into account the results demonstrated in table 7, and having already discarded 1L-16B-1MK, it is possible to conclude that the 1L-8B-2MK is the best combination, due to its lower average pressure drop along the system and reasonable standard deviation, followed by 1L-4B-4MK and 2L-4B-4MK, in this sequence, but the results are close enough for other factors, such as parts price, area available and transport logistics, to change the proposed option to the end client.

It can be concluded that the interpolations of loss coefficient at lower values of flow rate may be optimized, and that a high number of batteries of a single MK cyclone is not a proper combination to fulfil the requirements of the project at hand.

However, a further analysis with regards to heat transfer in the system would also give more input to conduct a more thorough study.

5 Conclusion

The main objective of this thesis was the design and parametrization (using a 3rd party software, like *Microsoft Excel*) of parts in *Autodesk Inventor* in order to automate the dimensions according to client's requirements.

The secondary objectives included assembling the designed parts into systems that should also be automated according to the input of the *Excel* spreadsheet; and export these values for pressure drop calculations, in order to also automate these, expediting and minimising the errors in the process. Using this way to calculate pressure drop, a study was conducted to determine the combination that would best suits a project for a new client.

While learning how to work in *Autodesk Inventor* was an arduous task, since there was no familiarity with the software, and even the basic concepts of modelling were not fully grasped, the objectives were fulfilled.

As such, comparing between 4 different combinations of 16 cyclones, it was concluded that, by pressure drop alone, the best solution was the 1L-8B-2MK with an average pressure drop of 2148.7 Pa, followed by 1L-4B-4MK and 2L-4B-4MK with an average pressure drop of 2197.5 Pa and 2216.4 Pa, respectively. The fourth combination was discarded, due to negative pressure drops, due to negative loss coefficient, implying that the interpolations are not correct for such a difference in flow rate. However, a further study including heat transfer in the system might help achieve more precise values.

By completing these tasks, both the designs and calculations of pressure drop were expedited, which, in turn, liberates some tasks and transforms other tasks from days to minutes. This allows the company to take on more contracts simultaneously, providing more exact models, while still providing customized projects.

6 Assessment of the work done

6.1 Objectives Achieved

For the realization of this work, some objectives were defined as goals: Design of parts in *Autodesk Inventor* and automation of parameters of those parts, using a *Microsoft Excel* spreadsheet linked to the parts file; Development and automation of the whole system - inlet pipeline, cyclone and outlet pipeline – using the same Excel spreadsheet; Export parameters values obtained to another spreadsheet and automate pressure drop calculations assuming all the paths a gaseous stream can take in all the layouts commercialized by ACS; using the automated calculations, check for the best solution for a new project, following the clients requirements. All these objectives, as defined, were fully accomplished.

6.2 Other Work Carried Out

Simultaneously with the work being made with the thesis in mind, there was a development of programming code in iLogic that is able to retrieve physical properties - area, volume, mass, etc - of all files in a project.

6.3 Limitations and Future Work

As of right now, all the parametrization and automations were made for parts that are used in the system. This means, if there is a need to add parts, it has to be designed, parametrized and linked to the current *Excel* spreadsheet.

For pressure drop calculations, as future work, the goal is to add heat transfer calculations, thus estimating a more precise fluid density value and, subsequently, a more precise pressure drop calculations. The algorithm is made and can be consulted in figure a.19 in the appendix. Seeing as there is already an iLogic code to retrieve all the areas of the parts in a project and export to *Excel*, the only thing missing right now is just the code development to implement the calculations in the Excel spreadsheet.

6.4 Final Assessment

It is my belief that the work developed in this master thesis is true added value for the company, since it can possibly relieve of days of work, allowing the company to work more projects simultaneously, while maintaining the same team and minimizing errors along all the workflow.

References

[1] Zhao, Bingtao & Shen, Henggen & Kang, Yanming. (2004). Development of a symmetrical spiral inlet to improve cyclone separator performance. Powder Technology. 145. 47-50. 10.1016/j.powtec.2004.06.001.

[2] Martignoni, Waldir & Bernardo, S & L. Quintani, C. (2007). Evaluation of cyclone geometry and its influence on performance parameters by computational fluid dynamics (CFD). Brazilian Journal of Chemical Engineering - BRAZ J CHEM ENG. 24. 10.1590/S0104-66322007000100008.

[3] Da Silva, Pascal & Briens, Cedric & Bernis, Alain. (2003). Development of a new rapid method to measure erosion rates in laboratory and pilot plant cyclones. Powder Technology - POWDER TECHNOL. 131. 111-119. 10.1016/S0032-5910(02)00338-8.

[4] Elsayed, Khairy & Lacor, C. (2010). Optimization of the cyclone separator geometry for minimum pressure drop using mathematical models and CFD simulations. Chemical Engineering Science. 65. 6048-6058. 10.1016/j.ces.2010.08.042.

[5] Solero, Giulio & Coghe, Aldo. (2002). Experimental fluid dynamic characterization of a cyclone chamber. Experimental Thermal and Fluid Science. 27. 87-96. 10.1016/S0894-1777(02)00221-2.

[6] Alves, André & Paiva, Julio & Salcedo, Romualdo. (2015). Cyclone optimization including particle clustering. Powder Technology. 272. 10.1016/j.powtec.2014.11.016.

[7] Yu, Jianfeng & Zhang, Ting & Qian, Jianming. (2011). Efficiency testing methods for centrifugal fans. Electrical Motor Products, 125–172. 10.1533/9780857093813.131.

[8] Gimbun, Jolius & Luqman Chuah, Abdullah & Fakhru'l-Razi, A & SY Choong, Thomas. (2005). The influence of temperature and inlet velocity on cyclone pressure drop: A CFD study. Chemical Engineering and Processing. 44. 7-12. 10.1016/j.cep.2004.03.005.

[9] American Society of Heating, Refrigerating and Air-Conditioning Engineers. (2001). *2001 ASHRAE handbook: Fundamentals*. Atlanta, GA: ASHRAE.

[10] Osborne, W.C. (1966). *Fans*. Pergamon Press Ltd., London.

[11] Ai, Z.T. & Mak, Cheuk Ming. (2013). Pressure Losses across Multiple Fittings in Ventilation Ducts. The Scientific World Journal. 2013. 195763. 10.1155/2013/195763.

[12] Colebrook, C. F. (1938). "Turbulent Flow in Pipes, With Particular Reference to the Transition Region Between the Smooth and Rough Pipe Laws". Journal of the Institution of Civil Engineers. London.

[13] História | ACSystems. (2019). Retrieved from https://www.advancedcyclonesystems.com/pt/historia. Accessed 29 Jun. 2019.

[14] Paiva, Julio. (2010). Captura de poeiras finas com ciclones de recirculação electrostática: conceptualização, modelização e validação experimental.

[15] Schmandt, Bastian & Herwig, Heinz. (2015). The head change coefficient for branched flows: Why “losses” due to junctions can be negative. International Journal of Heat and Fluid Flow. 54. 10.1016/j.ijheatfluidflow.2015.06.004.

Appendix

For all the parts involved in the system, the 2001 ASHRAE handbook [9] nomenclature was used. This terminology is displayed in table A.1. The suffix "_M" refers to the Main branch of the part and "_B" refers to the diverging or converging branch of the part.

Table A. 1 - ASHRAE handbook nomenclature. Adapted from 2001 ASHRAE handbook [9]

Part	Description
CD3-9	Elbow, 5 gore, with r/D = 1.5
ED4-1	Transition, Round to Round, Exhaust/Return Systems
ED4-2	Transition, Round to Rectangular, Exhaust/Return Systems
ED5-2	Converging 45° Wye - used as a converging 30° Wye
ED5-3	Converging 90° Wye, with Dc > 250 mm.
ED5-6	Capped converging Wye, Branch with 45° Elbow, Branch 90° to Main, r/Db = 1.5
ED5-9	Symmetrical Converging 60° Wye, $Db_1 \geq Db_2$
SD5-2	Diverging 45° Wye – used as a diverging 30° Wye
T-RET	Circular straight tube
T-RET_R	Rectangular straight tube

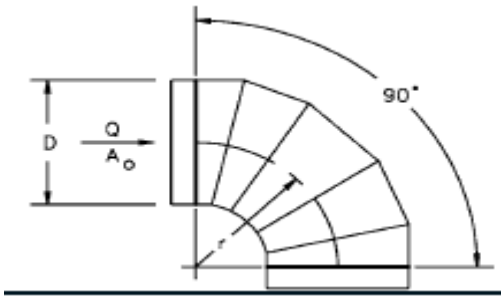


Figure A. 1 - CD3-9. Adapted from 2001 ASHRAE handbook [9]

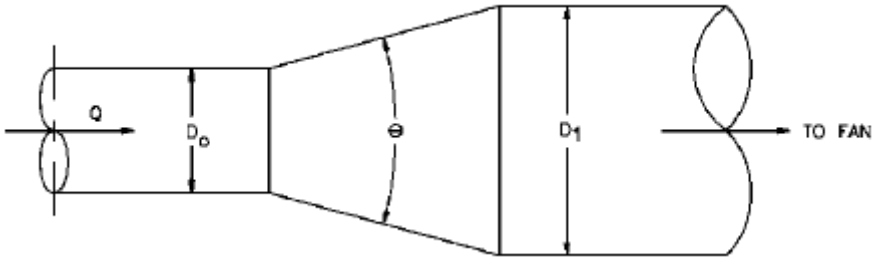


Figure A. 2 - ED4-1. Adapted from 2001 ASHRAE handbook [9]

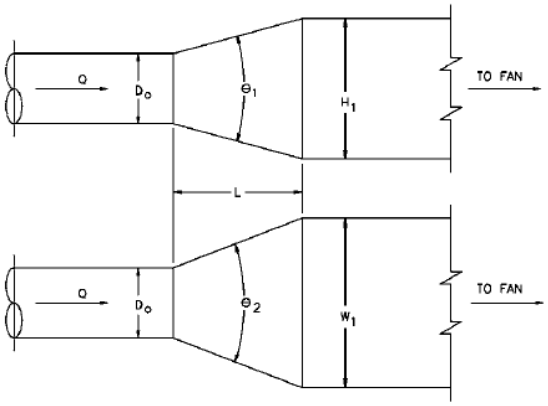


Figure A. 3 - ED4-2. Adapted from 2001 ASHRAE handbook [9]

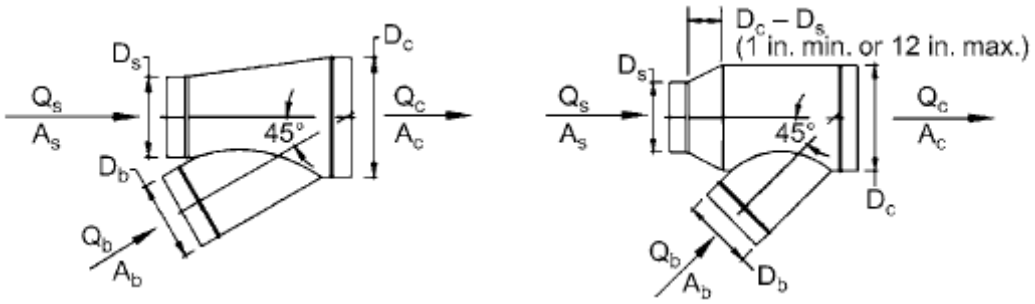


Figure A. 4 - ED5-2. Adapted from 2001 ASHRAE handbook [9]

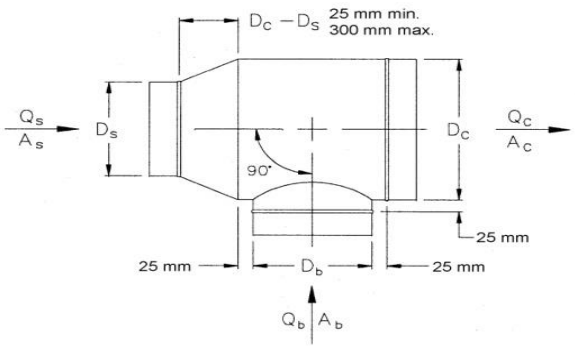


Figure A. 5 - ED5-3, DC > 250 mm. Adapted from 2001 ASHRAE handbook [9]

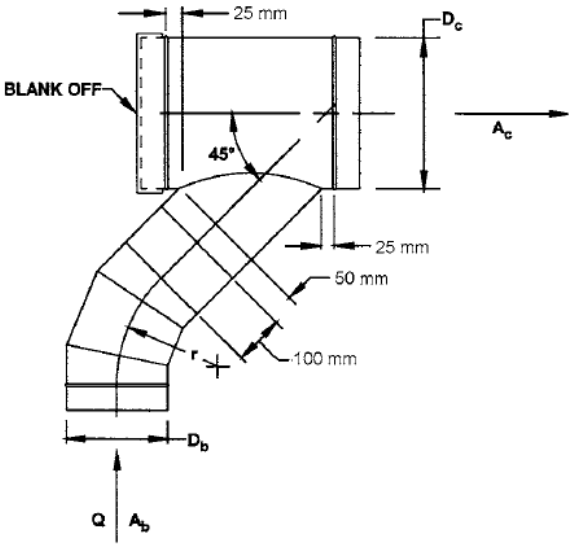


Figure A. 6 - ED5-6. Adapted from 2001 ASHRAE handbook [9]

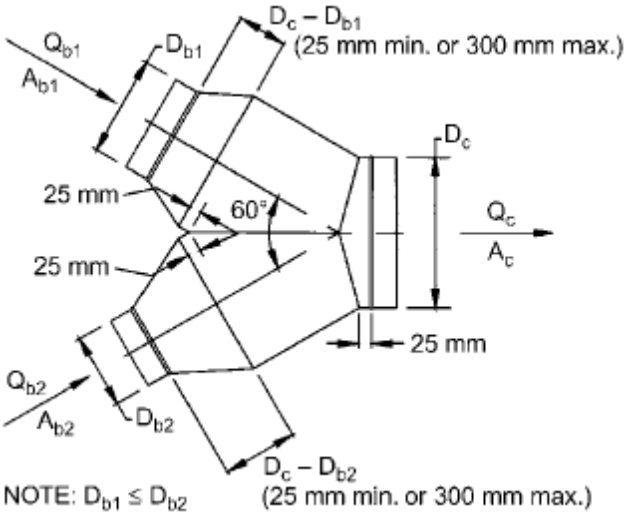


Figure A. 7 - ED5-9. Adapted from 2001 ASHRAE handbook [9]

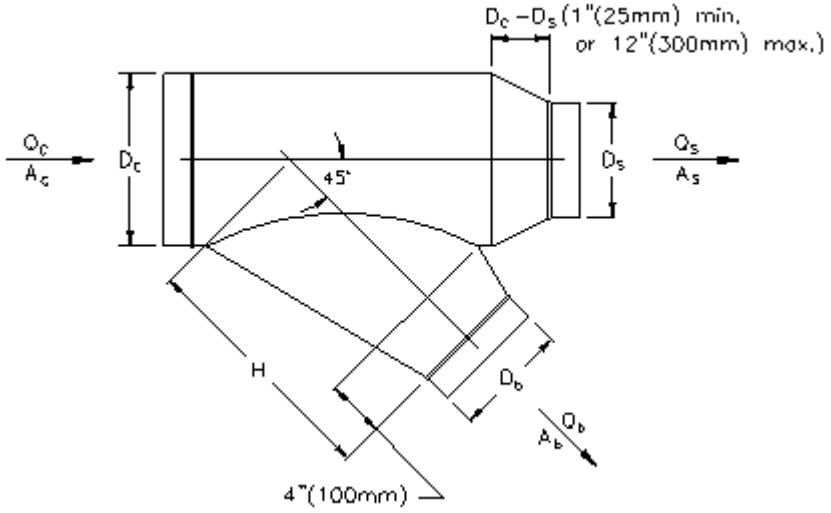


Figure A. 8 - SD5-2. Adapted from 2001 ASHRAE handbook [9]

Table A. 2 - Path taken by gas stream depending on cyclones in a 1L-16B-1MK arrange - cyclones 1 to 8

1	2	3	4	5	6	7	8
SD5-2_B	SD5-2_M	SD5-2_M	SD5-2_M	SD5-2_M	SD5-2_M	SD5-2_M	SD5-2_M
CD3-9	T-RET	T-RET	T-RET	T-RET	T-RET	T-RET	T-RET
ED4-2	SD5-2_B	SD5-2_M	SD5-2_M	SD5-2_M	SD5-2_M	SD5-2_M	SD5-2_M
CYCLONE	CD3-9	T-RET	T-RET	T-RET	T-RET	T-RET	T-RET
T-RET	T-RET	SD5-2_B	SD5-2_M	SD5-2_M	SD5-2_M	SD5-2_M	SD5-2_M
ED4-1	ED4-2	CD3-9	T-RET	T-RET	T-RET	T-RET	T-RET
T-RET	CYCLONE	T-RET	SD5-2_B	SD5-2_M	SD5-2_M	SD5-2_M	SD5-2_M
CD3-9	T-RET	ED4-2	CD3-9	T-RET	T-RET	T-RET	T-RET
T-RET	ED4-1	CYCLONE	T-RET	SD5-2_B	SD5-2_M	SD5-2_M	SD5-2_M
ED5-2_M	T-RET	T-RET	ED4-2	CD3-9	T-RET	T-RET	T-RET
T-RET	CD3-9	ED4-1	CYCLONE	T-RET	SD5-2_B	SD5-2_M	SD5-2_M
ED5-2_M	ED5-2_B	T-RET	T-RET	ED4-2	CD3-9	T-RET	T-RET
T-RET	T-RET	CD3-9	ED4-1	CYCLONE	T-RET	SD5-2_B	SD5-2_M
ED5-2_M	ED5-2_M	ED5-2_B	T-RET	T-RET	ED4-2	CD3-9	T-RET

T-RET	T-RET	T-RET	CD3-9	ED4-1	CYCLONE	T-RET	SD5-2_B
ED5-2_M	ED5-2_M	ED5-2_M	ED5-2_B	T-RET	T-RET	ED4-2	CD3-9
T-RET	T-RET	T-RET	T-RET	CD3-9	ED4-1	CYCLONE	T-RET
ED5-2_M	ED5-2_M	ED5-2_M	ED5-2_M	ED5-2_B	T-RET	T-RET	ED4-2
T-RET	T-RET	T-RET	T-RET	T-RET	CD3-9	ED4-1	CYCLONE
ED5-2_M	ED5-2_M	ED5-2_M	ED5-2_M	ED5-2_M	ED5-2_B	T-RET	T-RET
T-RET	T-RET	T-RET	T-RET	T-RET	T-RET	CD3-9	ED4-1
ED5-2_M	ED5-2_M	ED5-2_M	ED5-2_M	ED5-2_M	ED5-2_M	ED5-2_B	T-RET
T-RET	T-RET	T-RET	T-RET	T-RET	T-RET	T-RET	CD3-9
ED5-2_M	ED5-2_M	ED5-2_M	ED5-2_M	ED5-2_M	ED5-2_M	ED5-2_M	ED5-2_B
T-RET	T-RET	T-RET	T-RET	T-RET	T-RET	T-RET	T-RET
ED5-2_M	ED5-2_M	ED5-2_M	ED5-2_M	ED5-2_M	ED5-2_M	ED5-2_M	ED5-2_M
T-RET	T-RET	T-RET	T-RET	T-RET	T-RET	T-RET	T-RET
ED5-2_M	ED5-2_M	ED5-2_M	ED5-2_M	ED5-2_M	ED5-2_M	ED5-2_M	ED5-2_M
T-RET	T-RET	T-RET	T-RET	T-RET	T-RET	T-RET	T-RET
ED5-2_M	ED5-2_M	ED5-2_M	ED5-2_M	ED5-2_M	ED5-2_M	ED5-2_M	ED5-2_M
T-RET	T-RET	T-RET	T-RET	T-RET	T-RET	T-RET	T-RET
ED5-2_M	ED5-2_M	ED5-2_M	ED5-2_M	ED5-2_M	ED5-2_M	ED5-2_M	ED5-2_M
T-RET	T-RET	T-RET	T-RET	T-RET	T-RET	T-RET	T-RET
ED5-2_M	ED5-2_M	ED5-2_M	ED5-2_M	ED5-2_M	ED5-2_M	ED5-2_M	ED5-2_M
T-RET	T-RET	T-RET	T-RET	T-RET	T-RET	T-RET	T-RET
ED5-2_M	ED5-2_M	ED5-2_M	ED5-2_M	ED5-2_M	ED5-2_M	ED5-2_M	ED5-2_M
T-RET	T-RET	T-RET	T-RET	T-RET	T-RET	T-RET	T-RET
	ED5-2_M	ED5-2_M	ED5-2_M	ED5-2_M	ED5-2_M	ED5-2_M	ED5-2_M
	T-RET	T-RET	T-RET	T-RET	T-RET	T-RET	T-RET

Table A. 3 - Path taken by gas stream depending on cyclones in a 1L-16B-1MK arrange - cyclones 9 to 16

9	10	11	12	13	14	15	16
SD5-2_M	SD5-2_M	SD5-2_M	SD5-2_M	SD5-2_M	SD5-2_M	SD5-2_M	SD5-2_M
T-RET	T-RET	T-RET	T-RET	T-RET	T-RET	T-RET	T-RET
SD5-2_M	SD5-2_M	SD5-2_M	SD5-2_M	SD5-2_M	SD5-2_M	SD5-2_M	SD5-2_M
T-RET	T-RET	T-RET	T-RET	T-RET	T-RET	T-RET	T-RET
SD5-2_M	SD5-2_M	SD5-2_M	SD5-2_M	SD5-2_M	SD5-2_M	SD5-2_M	SD5-2_M
T-RET	T-RET	T-RET	T-RET	T-RET	T-RET	T-RET	T-RET
SD5-2_M	SD5-2_M	SD5-2_M	SD5-2_M	SD5-2_M	SD5-2_M	SD5-2_M	SD5-2_M
T-RET	T-RET	T-RET	T-RET	T-RET	T-RET	T-RET	T-RET
SD5-2_M	SD5-2_M	SD5-2_M	SD5-2_M	SD5-2_M	SD5-2_M	SD5-2_M	SD5-2_M
T-RET	T-RET	T-RET	T-RET	T-RET	T-RET	T-RET	T-RET
SD5-2_M	SD5-2_M	SD5-2_M	SD5-2_M	SD5-2_M	SD5-2_M	SD5-2_M	SD5-2_M
T-RET	T-RET	T-RET	T-RET	T-RET	T-RET	T-RET	T-RET
SD5-2_M	SD5-2_M	SD5-2_M	SD5-2_M	SD5-2_M	SD5-2_M	SD5-2_M	SD5-2_M
T-RET	T-RET	T-RET	T-RET	T-RET	T-RET	T-RET	T-RET
SD5-2_M	SD5-2_M	SD5-2_M	SD5-2_M	SD5-2_M	SD5-2_M	SD5-2_M	SD5-2_M
T-RET	T-RET	T-RET	T-RET	T-RET	T-RET	T-RET	T-RET
SD5-2_B	SD5-2_M	SD5-2_M	SD5-2_M	SD5-2_M	SD5-2_M	SD5-2_M	SD5-2_M
CD3-9	T-RET	T-RET	T-RET	T-RET	T-RET	T-RET	T-RET
T-RET	SD5-2_B	SD5-2_M	SD5-2_M	SD5-2_M	SD5-2_M	SD5-2_M	SD5-2_M
ED4-2	CD3-9	T-RET	T-RET	T-RET	T-RET	T-RET	T-RET
CYCLONE	T-RET	SD5-2_B	SD5-2_M	SD5-2_M	SD5-2_M	SD5-2_M	SD5-2_M
T-RET	ED4-2	CD3-9	T-RET	T-RET	T-RET	T-RET	T-RET
ED4-1	CYCLONE	T-RET	SD5-2_B	SD5-2_M	SD5-2_M	SD5-2_M	SD5-2_M
T-RET	T-RET	ED4-2	CD3-9	T-RET	T-RET	T-RET	T-RET

CD3-9	ED4-1	CYCLONE	T-RET	SD5-2_B	SD5-2_M	SD5-2_M	SD5-2_M
ED5-2_B	T-RET	T-RET	ED4-2	CD3-9	T-RET	T-RET	T-RET
T-RET	CD3-9	ED4-1	CYCLONE	T-RET	SD5-2_B	SD5-2_M	SD5-2_M
ED5-2_M	ED5-2_B	T-RET	T-RET	ED4-2	CD3-9	T-RET	T-RET
T-RET	T-RET	CD3-9	ED4-1	CYCLONE	T-RET	SD5-2_B	SD5-2_M
ED5-2_M	ED5-2_M	ED5-2_B	T-RET	T-RET	ED4-2	CD3-9	T-RET
T-RET	T-RET	T-RET	CD3-9	ED4-1	CYCLONE	T-RET	CD3-9
ED5-2_M	ED5-2_M	ED5-2_M	ED5-2_B	T-RET	T-RET	ED4-2	T-RET
T-RET	T-RET	T-RET	T-RET	CD3-9	ED4-1	CYCLONE	ED4-2
ED5-2_M	ED5-2_M	ED5-2_M	ED5-2_M	ED5-2_B	T-RET	T-RET	CYCLONE
T-RET	T-RET	T-RET	T-RET	T-RET	CD3-9	ED4-1	T-RET
ED5-2_M	ED5-2_M	ED5-2_M	ED5-2_M	ED5-2_M	ED5-2_B	T-RET	ED4-1
T-RET	T-RET	T-RET	T-RET	T-RET	T-RET	CD3-9	CD3-9
ED5-2_M	ED5-2_M	ED5-2_M	ED5-2_M	ED5-2_M	ED5-2_M	ED5-2_B	ED5-2_B
T-RET	T-RET	T-RET	T-RET	T-RET	T-RET	T-RET	T-RET
ED5-2_M	ED5-2_M	ED5-2_M	ED5-2_M	ED5-2_M	ED5-2_M	ED5-2_M	
T-RET	T-RET	T-RET	T-RET	T-RET	T-RET	T-RET	

Table A. 4 - Path taken by gas stream depending on cyclones in a 1L-8B-2MK arrange

1	2	3	4	5	6	7	8
SD5-2_B	SD5-2_M	SD5-2_M	SD5-2_M	SD5-2_M	SD5-2_M	SD5-2_M	SD5-2_M
CD3-9	T-RET	T-RET	T-RET	T-RET	T-RET	T-RET	T-RET
ED4-2	SD5-2_B	SD5-2_M	SD5-2_M	SD5-2_M	SD5-2_M	SD5-2_M	SD5-2_M
CYCLONE	CD3-9	T-RET	T-RET	T-RET	T-RET	T-RET	T-RET
T-RET	T-RET	SD5-2_B	SD5-2_M	SD5-2_M	SD5-2_M	SD5-2_M	SD5-2_M
ED4-1	ED4-2	CD3-9	T-RET	T-RET	T-RET	T-RET	T-RET
CD3-9	CYCLONE	T-RET	SD5-2_B	SD5-2_M	SD5-2_M	SD5-2_M	SD5-2_M

CD3-9	T-RET	ED4-2	CD3-9	T-RET	T-RET	T-RET	T-RET
CD3-9	ED4-1	CYCLONE	T-RET	SD5-2_B	SD5-2_M	SD5-2_M	SD5-2_M
ED5-9_B	CD3-9	T-RET	ED4-2	CD3-9	T-RET	T-RET	T-RET
T-RET	CD3-9	ED4-1	CYCLONE	T-RET	SD5-2_B	SD5-2_M	SD5-2_M
CD3-9	CD3-9	CD3-9	T-RET	ED4-2	CD3-9	T-RET	T-RET
T-RET	ED5-9_B	CD3-9	ED4-1	CYCLONE	T-RET	SD5-2_B	SD5-2_M
ED5-2_M	T-RET	CD3-9	CD3-9	T-RET	ED4-2	CD3-9	T-RET
T-RET	CD3-9	ED5-9_B	CD3-9	ED4-1	CYCLONE	T-RET	CD3-9
ED5-2_M	ED5-2_B	T-RET	CD3-9	CD3-9	T-RET	ED4-2	T-RET
T-RET	T-RET	CD3-9	ED5-9_B	CD3-9	ED4-1	CYCLONE	ED4-2
ED5-2_M	ED5-2_M	ED5-2_B	T-RET	CD3-9	CD3-9	T-RET	CYCLONE
T-RET	T-RET	T-RET	CD3-9	ED5-9_B	CD3-9	ED4-1	T-RET
ED5-2_M	ED5-2_M	ED5-2_M	ED5-2_B	T-RET	CD3-9	CD3-9	ED4-1
T-RET	T-RET	T-RET	T-RET	CD3-9	ED5-9_B	CD3-9	CD3-9
ED5-2_M	ED5-2_M	ED5-2_M	ED5-2_M	ED5-2_B	T-RET	CD3-9	CD3-9
T-RET	T-RET	T-RET	T-RET	T-RET	CD3-9	ED5-9_B	CD3-9
ED5-2_M	ED5-2_M	ED5-2_M	ED5-2_M	ED5-2_M	ED5-2_B	T-RET	ED5-9_B
T-RET	T-RET	T-RET	T-RET	T-RET	T-RET	CD3-9	CD3-9
ED5-2_M	ED5-2_M	ED5-2_M	ED5-2_M	ED5-2_M	ED5-2_M	ED5-2_B	ED5-2_B
T-RET	T-RET	T-RET	T-RET	T-RET	T-RET	T-RET	T-RET
	ED5-2_M	ED5-2_M	ED5-2_M	ED5-2_M	ED5-2_M	ED5-2_M	
	T-RET	T-RET	T-RET	T-RET	T-RET	T-RET	

Table A. 5 - Path taken by gas stream depending on cyclones in a 1L-4B-4MK arrange

1	2	3	4	5	6	7	8
SD5-2_B	SD5-2_B	SD5-2_M	SD5-2_M	SD5-2_M	SD5-2_M	SD5-2_M	SD5-2_M
CD3-9	CD3-9	T-RET	T-RET	T-RET	T-RET	T-RET	T-RET
ED4-2	ED4-2	SD5-2_B	SD5-2_B	SD5-2_M	SD5-2_M	SD5-2_M	SD5-2_M
CYCLONE	T-RET_R	CD3-9	CD3-9	T-RET	T-RET	T-RET	T-RET
T-RET	CYCLONE	T-RET	T-RET	SD5-2_B	SD5-2_B	SD5-2_M	SD5-2_M
ED4-1	T-RET	ED4-2	ED4-2	CD3-9	CD3-9	T-RET	T-RET
ED5-6	ED4-1	CYCLONE	T-RET_R	T-RET	T-RET	CD3-9	CD3-9
ED5-3_M	ED5-3_B	T-RET	CYCLONE	ED4-2	ED4-2	T-RET	T-RET
ED4-1	ED4-1	ED4-1	T-RET	CYCLONE	T-RET_R	ED4-2	ED4-2
CD3-9	CD3-9	ED5-6	ED4-1	T-RET	CYCLONE	CYCLONE	T-RET_R
ED5-9_B	ED5-9_B	ED5-3_M	ED5-3_B	ED4-1	T-RET	T-RET	CYCLONE
T-RET	T-RET	ED4-1	ED4-1	ED5-6	ED4-1	ED4-1	T-RET
CD3-9	CD3-9	CD3-9	CD3-9	ED5-3_M	ED5-3_B	ED5-6	ED4-1
T-RET	T-RET	ED5-9_B	ED5-9_B	ED4-1	ED4-1	ED5-3_M	ED5-3_B
ED5-2_M	ED5-2_M	T-RET	T-RET	CD3-9	CD3-9	ED4-1	ED4-1
T-RET	T-RET	CD3-9	CD3-9	ED5-9_B	ED5-9_B	CD3-9	CD3-9
ED5-2_M	ED5-2_M	ED5-2_B	ED5-2_B	T-RET	T-RET	ED5-9_B	ED5-9_B
T-RET	T-RET	T-RET	T-RET	CD3-9	CD3-9	CD3-9	CD3-9
ED5-2_M	ED5-2_M	ED5-2_M	ED5-2_M	ED5-2_B	ED5-2_B	ED5-2_B	ED5-2_B
T-RET	T-RET	T-RET	T-RET	T-RET	T-RET	T-RET	T-RET
		ED5-2_M	ED5-2_M	ED5-2_M	ED5-2_M		
		T-RET	T-RET	T-RET	T-RET		

Table A. 6 - Path taken by gas stream depending on cyclones in a 2L-4B-4MK

1	2	3	4	5	6	7	8
SD5-2_B	SD5-2_B	SD5-2_B	SD5-2_B	SD5-2_M	SD5-2_M	SD5-2_M	SD5-2_M
CD3-9	CD3-9	CD3-9	CD3-9	T-RET	T-RET	T-RET	T-RET
ED4-2	ED4-2	ED4-2	ED4-2	CD3-9	CD3-9	CD3-9	CD3-9
CYCLONE	T-RET_R	T-RET_R	T-RET_R	T-RET	T-RET	T-RET	T-RET
T-RET	CYCLONE	T-RET_R	T-RET_R	ED4-2	ED4-2	ED4-2	ED4-2
ED4-1	T-RET	CYCLONE	CYCLONE	CYCLONE	T-RET_R	T-RET_R	T-RET_R
ED5-6	ED4-1	T-RET	T-RET	T-RET	CYCLONE	T-RET_R	T-RET_R
ED5-3_M	ED5-3_B	ED4-1	ED4-1	ED4-1	T-RET	CYCLONE	CYCLONE
ED5-3_M	ED5-3_M	ED5-3_B	ED5-3_B	ED5-6	ED4-1	T-RET	T-RET
ED5-3_M	ED5-3_M	ED5-3_M	ED4-1	ED5-3_M	ED5-3_B	ED4-1	ED4-1
ED4-1	ED4-1	ED4-1	CD3-9	ED5-3_M	ED5-3_M	ED5-3_B	ED5-3_B
CD3-9	CD3-9	CD3-9	CD3-9	ED5-3_M	ED5-3_M	ED5-3_M	ED4-1
CD3-9	CD3-9	CD3-9	ED5-9_B	ED4-1	ED4-1	ED4-1	CD3-9
ED5-9_B	ED5-9_B	ED5-9_B	T-RET	CD3-9	CD3-9	CD3-9	CD3-9
T-RET	T-RET	T-RET	CD3-9	CD3-9	CD3-9	CD3-9	ED5-9_B
CD3-9	CD3-9	CD3-9	T-RET	ED5-9_B	ED5-9_B	ED5-9_B	CD3-9
T-RET	T-RET	T-RET	ED5-2_M	CD3-9	CD3-9	CD3-9	ED5-2_B
ED5-2_M	ED5-2_M	ED5-2_M	T-RET	ED5-2_B	ED5-2_B	ED5-2_B	T-RET
T-RET	T-RET	T-RET		T-RET	T-RET	T-RET	

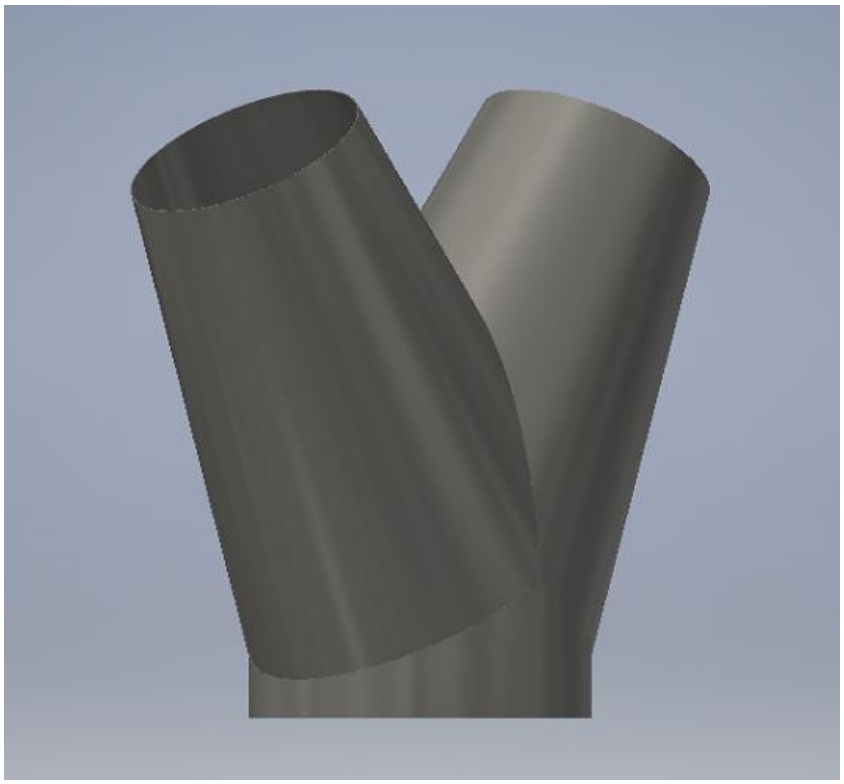


Figure A. 9 – Wye (ED5-9)

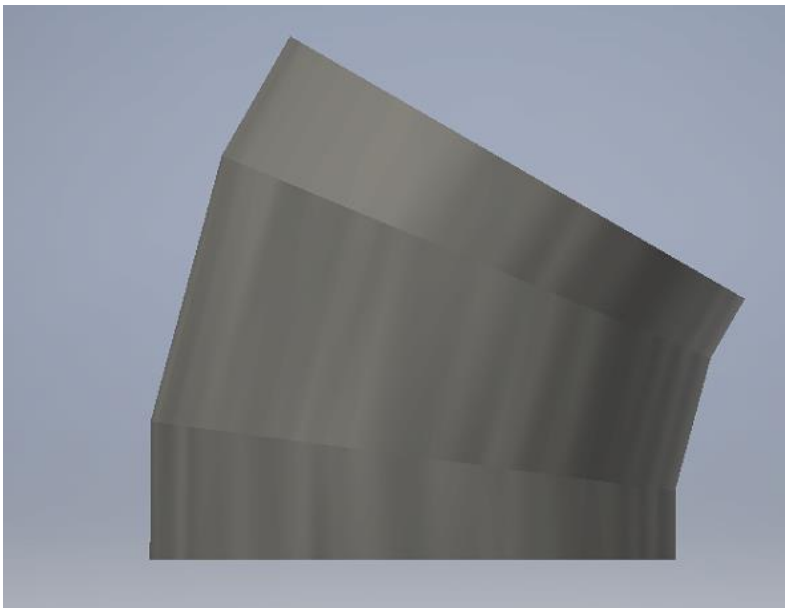


Figure A. 10 – 30° elbow (CD3-9)

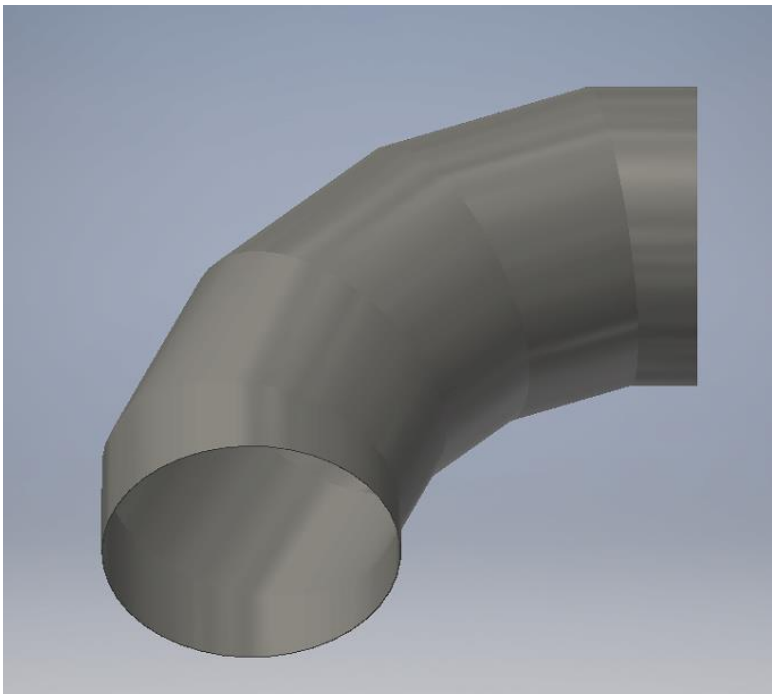


Figure A. 11 - 90° elbow (CD3-9)

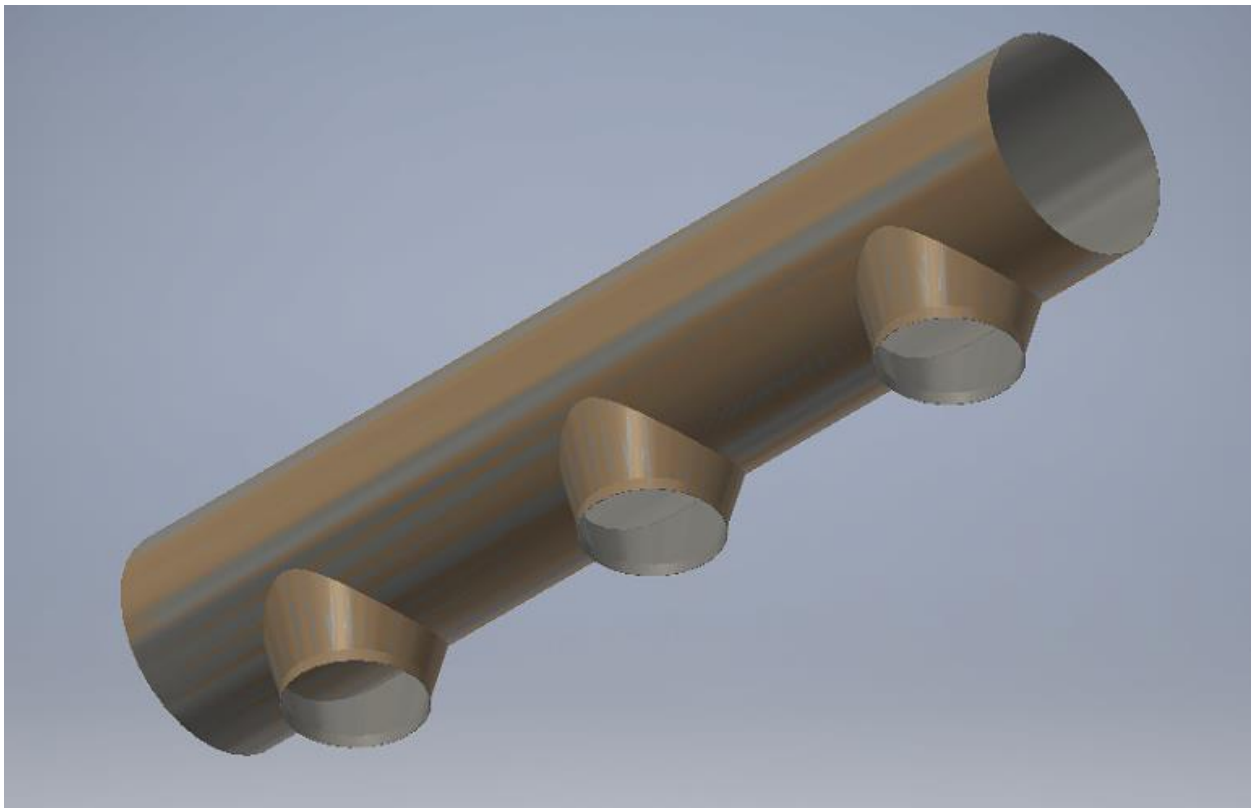


Figure A. 12 - Overhead collector for a battery comprised of 6 cyclones

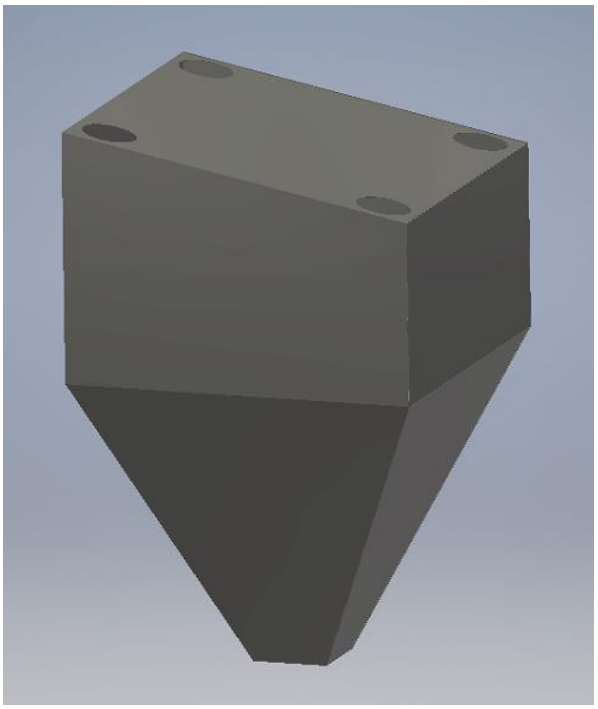


Figure A. 13 - Dust collector for a battery comprised of 4 cyclones

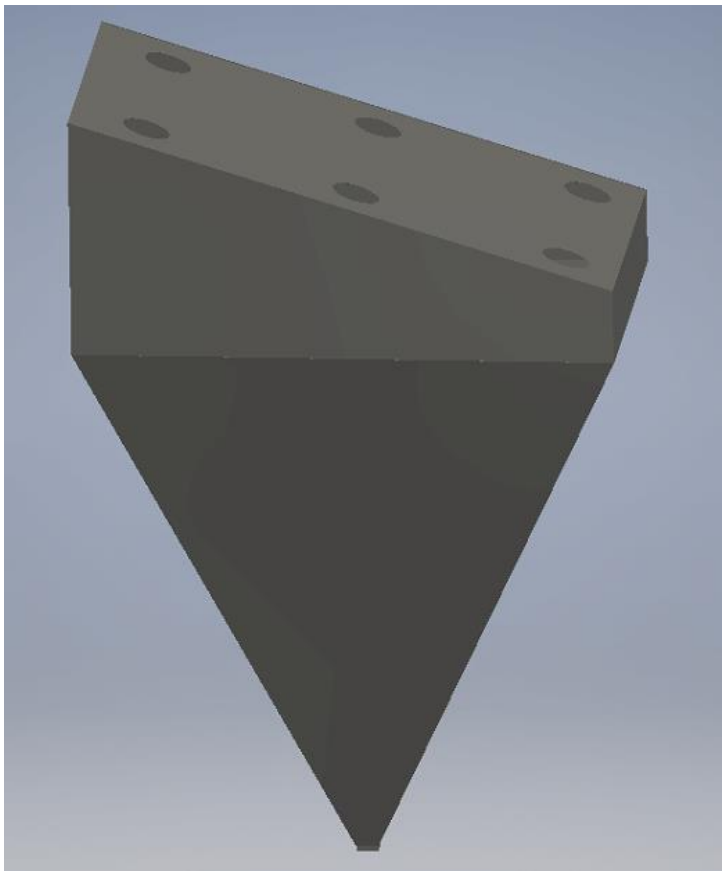


Figure A. 14 - Dust collector for a battery comprised of 6 cyclones

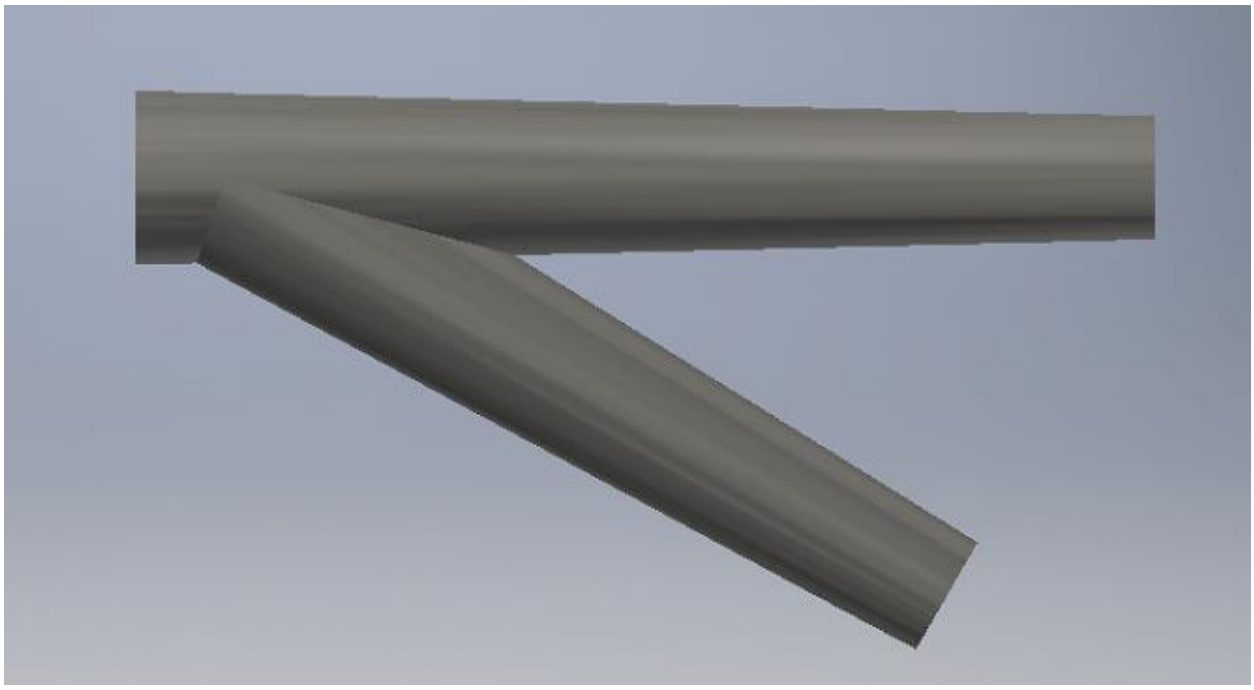


Figure A. 15 - Diverging 30° Wye (SD5-2)

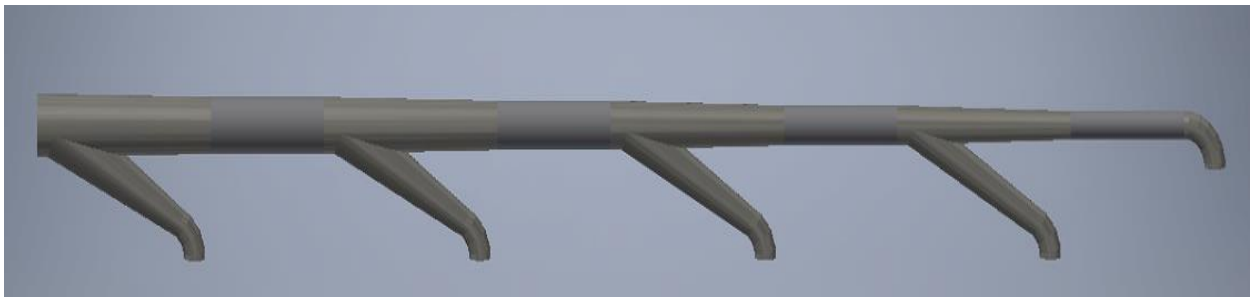


Figure A. 16 - Example of inlet pipelines

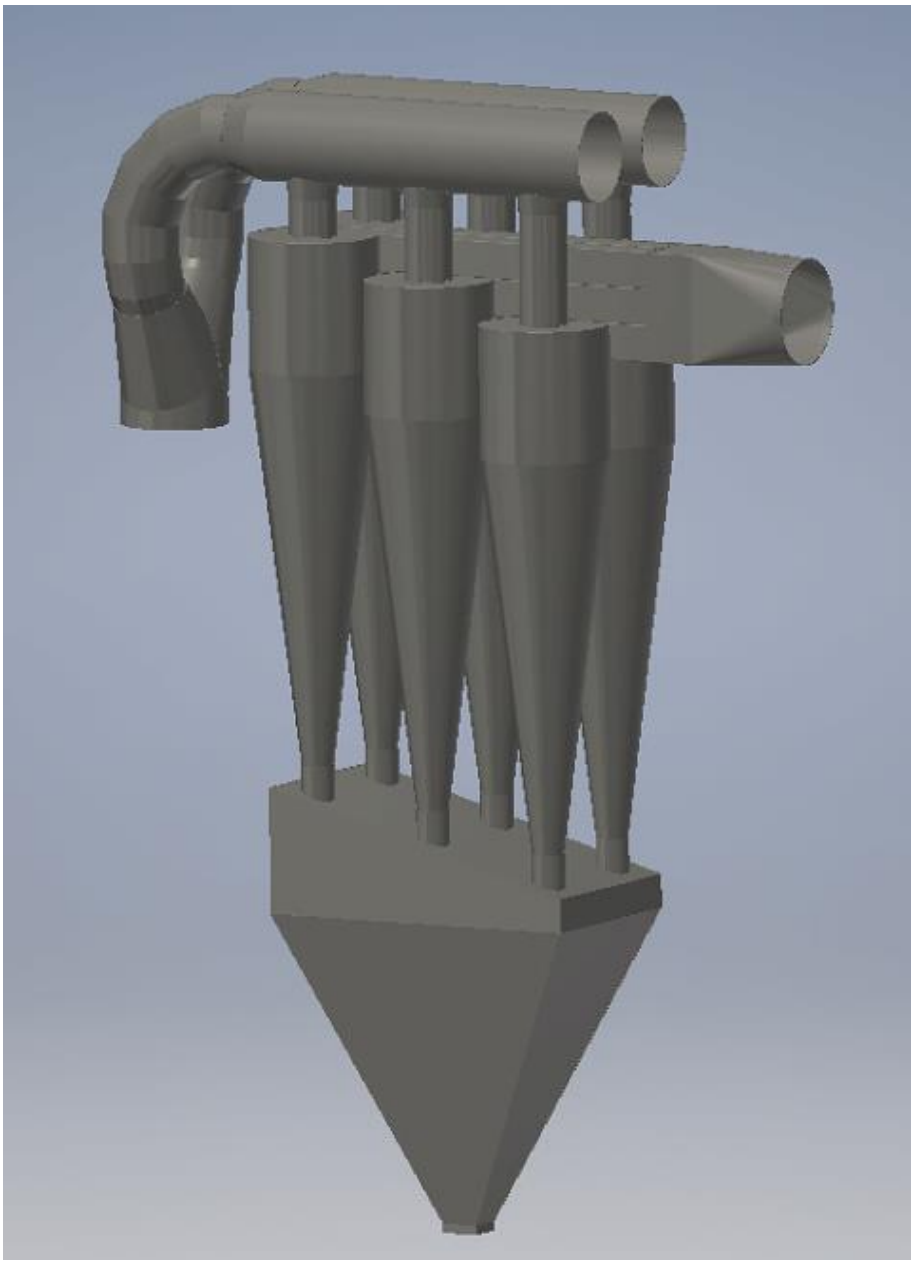


Figure A. 17 - Battery of 6 cyclones

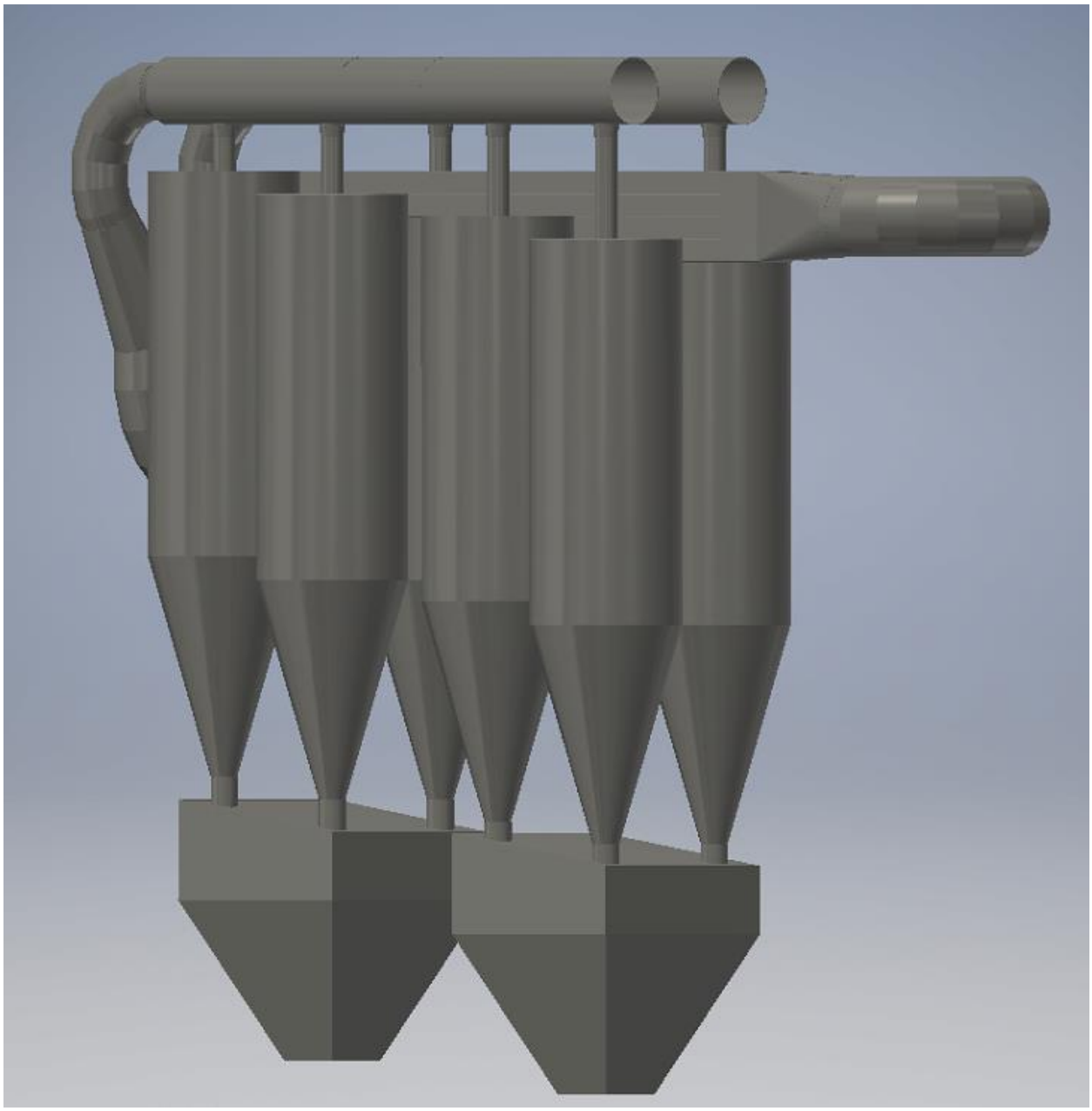


Figure A. 18 - 2L-2B-4MK layout

Table A. 7 - Path 1 of 2L-4B-4MK combination - parts geometry

Part	R_Q	$\dot{m}$ (kg/h)	Geometry				
SD5-2_B	1	14889	dc (mm) = 665	ds (mm) = 470		db (mm) = 470	
CD3-9	0.5	7445	d (mm) = 470				
ED4-2	0.5	7445	l (mm) = 610	d0 (mm) = 470	h (mm) = 130	w (mm) = 130	Angle = 19
T-RET_R	0.0625	931	l (m) = 0.906	h (mm) = 130	w (mm) = 130	eps (m) = 6×10^{-5}	Dh (mm) = 130

CYCLONE	0.0625	931	d (mm) = 128.7				
T-RET	0.0625	931	l (m) = 0.4249	d (mm) = 129		eps (m) = 6 x 10^{-5}	
ED4-1	0.0625	931	l (mm) = 75	d0 (mm) = 129	d1 (mm) = 233		Angle = 15
ED5-3_B	0.0625	931	db (mm) = 233	ds (mm) = 397		dc (mm) = 397	
ED5-3_M	0.125	1861	ds (mm) = 397	db (mm) = 233		dc (mm) = 397	
ED5-3_M	0.1875	2792	ds (mm) = 397	db (mm) = 233		dc (mm) = 397	
ED4-1	0.25	3722	l (mm) = 89	d0 (mm) = 397	d1 (mm) = 332		Angle = 20
CD3-9	0.25	3722	Angle = 90	d (mm) = 332			
CD3-9	0.25	3722	Angle = 30	d (mm) = 332			
ED5-9_B	0.25	3722	db1 (mm) = 332		db2 (mm) = 332	dc (mm) = 470	
CD3-9	0.5	7445	Angle = 90	d (mm) = 470			
T-RET	0.5	7445	l(m) = 2	d (mm) = 470		eps (m) = 6 x 10^{-5}	
ED5-2_M	0.5	7445	ds (mm) = 470		db (mm) = 470	dc (mm) = 665	
T-RET	1	14889	l (m) = 0.5	d (mm) = 665		eps (m) = 6 x 10^{-5}	

Table A. 8 - Path 1 of 2L-4B-4MK layout - iteration 1

Part	ρ (kg/m^3)	μ (Pa.s)	Q (m^3/h)	v (m/s)	k	Δp (Pa)	P (Pa)
SD5-2_B	0.5955594	2.92E-05	25000	20.000	0.1500	17.87	101307
CD3-9	0.5954544	2.92E-05	12502	20.004	0.1150	13.70	101293
ED4-2	0.5953738	2.92E-05	12504	20.006	0.4275	50.94	101242
T-RET_R	0.5950742	2.92E-05	1564	25.719	0.0319	6.28	101236
GEN	0.5950408	2.92E-05	1564	33.392	5.5000	1824.64	99412
T-RET	0.5841193	2.92E-05	1593	34.017	0.0299	10.11	99368
ED4-1	0.5840903	2.92E-05	1593	34.019	0.1925	65.07	99309
ED5-3_B	0.5837076	2.92E-05	1594	10.370	0.9133	28.66	99280
ED5-3_M	0.5835391	2.92E-05	3189	7.144	0.7537	11.22	99269
ED5-3_M	0.5834731	2.92E-05	4785	10.718	0.4333	14.52	99254

ED4-1	0.5833878	2.92E-05	6380	14.292	0.0814	4.85	99249
CD3-9	0.5833593	2.92E-05	6381	20.418	0.1719	20.90	99228
CD3-9	0.5832364	2.92E-05	6382	20.423	0.0773	9.41	99219
ED5-9_B	0.5831811	2.92E-05	6383	20.425	0.3200	38.92	99180
CD3-9	0.5829522	2.92E-05	12770	20.433	0.1475	17.95	99162
T-RET	0.5828467	2.92E-05	12773	20.436	0.0184	2.23	99160
ED5-2_M	0.5828204	2.92E-05	12773	20.433	0.2099	25.54	99132
T-RET	0.5826702	2.92E-05	25553	20.443	0.0159	1.94	99130

Table A. 9 - Path 1 of 2L-4B-4MK layout – iteration 2

Part	ρ (kg/m^3)	μ (Pa.s)	Q (m^3/h)	v (m/s)	k	Δp (Pa)	P (Pa)
SD5-2_B	0.5954544	2.92E-05	25004	20.004	0.1500	17.87	101307
CD3-9	0.5953738	2.92E-05	12504	20.006	0.1150	13.71	101293
ED4-2	0.5950744	2.92E-05	12510	20.016	0.4275	50.96	101242
T-RET_R	0.5950374	2.92E-05	1564	25.720	0.0319	5.69	101237
GEN	0.5843161	2.92E-05	1593	34.005	5.5000	1858.13	99379
T-RET	0.5840562	2.92E-05	1593	34.021	0.0299	4.30	99374
ED4-1	0.5837079	2.92E-05	1594	34.041	0.1925	65.11	99309
ED5-3_B	0.5835392	2.92E-05	1595	10.373	0.9133	28.67	99280
ED5-3_M	0.5834732	2.92E-05	3190	7.145	0.7537	11.22	99269
ED5-3_M	0.5833878	2.92E-05	4785	10.719	0.4333	14.52	99254
ED4-1	0.5833593	2.92E-05	6381	14.293	0.0814	4.85	99249
CD3-9	0.5832364	2.92E-05	6382	20.423	0.1719	20.91	99228
CD3-9	0.5831811	2.92E-05	6383	20.425	0.0773	9.41	99219
ED5-9_B	0.5829523	2.92E-05	6385	20.433	0.3200	38.94	99180
CD3-9	0.5828467	2.92E-05	12773	20.436	0.1475	17.95	99162
T-RET	0.5828336	2.92E-05	12773	20.437	0.0184	4.48	99158
ED5-2_M	0.5826702	2.92E-05	12777	20.439	0.2099	25.55	99132
T-RET	0.5826588	2.92E-05	25554	20.443	0.0159	0.97	99131

Table A. 10 - Path 1 of 2L-4B-4MK layout - iteration 3

Part	ρ (kg/m^3)	μ (Pa.s)	Q (m^3/h)	v (m/s)	k	Δp (Pa)	P (Pa)	error
SD5-2_B	0.5954544	2.92E-05	25004	20.004	0.1500	17.87	101307	3.4E-16
CD3-9	0.5953738	2.92E-05	12504	20.006	0.1150	13.71	101293	1.2E-16
ED4-2	0.5950742	2.92E-05	12510	20.016	0.4275	50.96	101242	2.3E-14
T-RET_R	0.5950408	2.92E-05	1564	25.720	0.0319	5.69	101237	1.2E-11
GEN	0.5841193	2.92E-05	1593	34.017	5.5000	1858.76	99378	3.9E-08
T-RET	0.5840903	2.92E-05	1593	34.019	0.0299	4.30	99374	1.2E-09
ED4-1	0.5837076	2.92E-05	1594	34.041	0.1925	65.11	99309	6.3E-14
ED5-3_B	0.5835391	2.92E-05	1595	10.373	0.9133	28.67	99280	2.4E-15
ED5-3_M	0.5834731	2.92E-05	3190	7.145	0.7537	11.22	99269	5.6E-17
ED5-3_M	0.5833878	2.92E-05	4785	10.719	0.4333	14.52	99254	1.6E-16
ED4-1	0.5833593	2.92E-05	6381	14.293	0.0814	4.85	99249	1.9E-18
CD3-9	0.5832364	2.92E-05	6382	20.423	0.1719	20.91	99228	6.7E-16
CD3-9	0.5831811	2.92E-05	6383	20.425	0.0773	9.41	99219	2.7E-17
ED5-9_B	0.5829522	2.92E-05	6385	20.433	0.3200	38.94	99180	8.1E-15
CD3-9	0.5828467	2.92E-05	12773	20.436	0.1475	17.95	99162	3.6E-16
T-RET	0.5828204	2.92E-05	12773	20.437	0.0184	4.48	99158	1.7E-10
ED5-2_M	0.5826702	2.92E-05	12777	20.439	0.2099	25.55	99132	1.5E-15
T-RET	0.5826645	2.92E-05	25553	20.443	0.0159	0.97	99131	3.2E-11

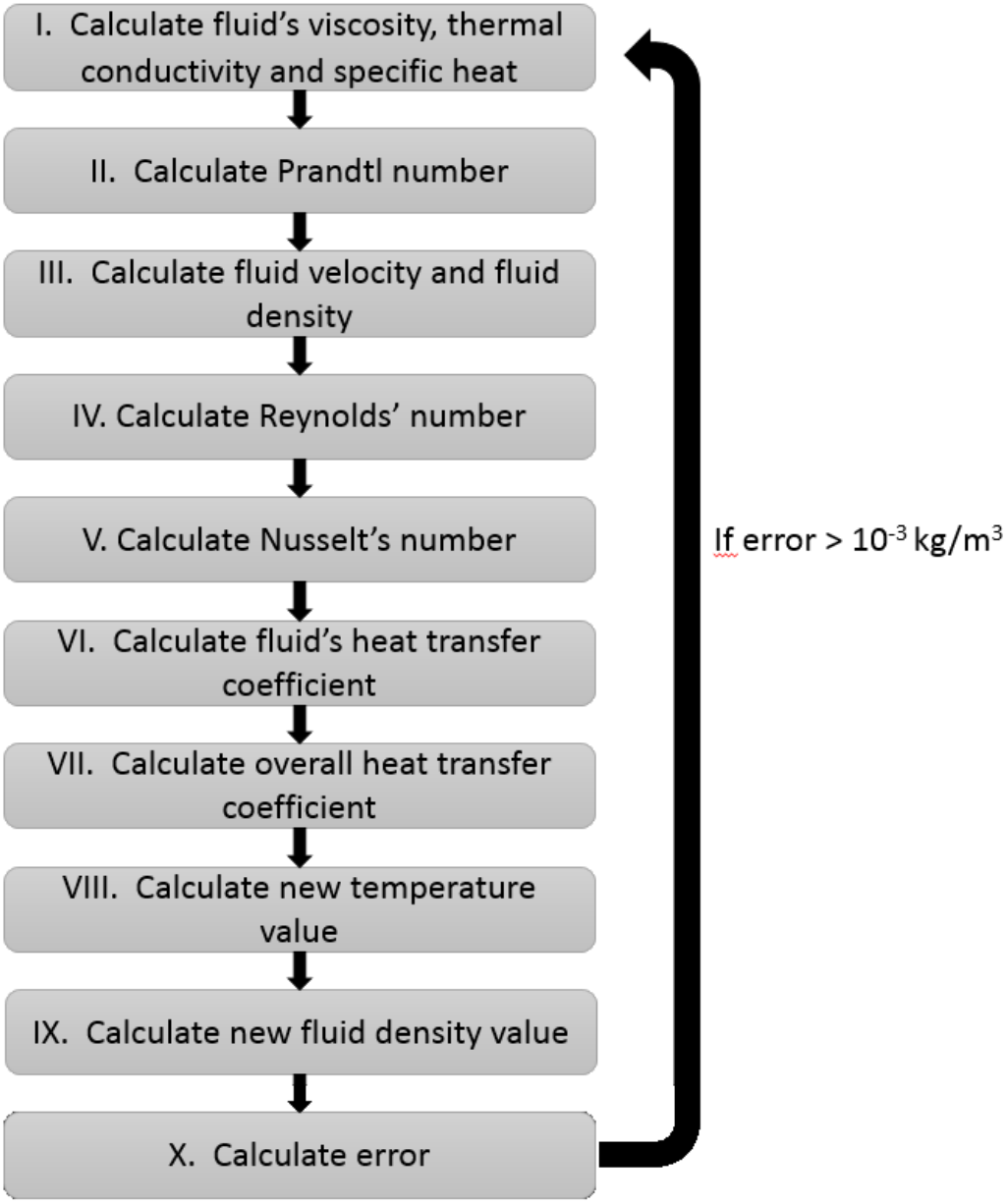


Figure A. 19 - Heat Transfer algorithm